

# SUPPORTING INFORMATION FOR

## Developing Hyperpolarized Butane Gas for Ventilation

### Lung Imaging

Nuwandi M. Ariyasingha\*,<sup>a</sup> Anna Samoilenko,<sup>a</sup> Md Raduanul H. Chowdhury,<sup>a</sup> Shiraz Nantogma,<sup>a</sup> Clementinah Oladun,<sup>a</sup> Jonathan R. Birchall,<sup>a</sup> Tarek Bawardi,<sup>a</sup> Oleg G. Salnikov,<sup>b,c</sup> Larisa M. Kovtunova,<sup>b,c</sup> Valerii I. Bukhtiyarov,<sup>c</sup> Zhongjie Shi,<sup>d</sup> Kehuan Luo,<sup>d</sup> Sidhartha Tan,<sup>d</sup> Igor V. Koptuyug,<sup>b</sup> Boyd M. Goodson,<sup>e</sup> Eduard Y. Chekmenev\*

<sup>a</sup> Department of Chemistry, Karmanos Cancer Institute (KCI), Integrative Biosciences (Ibio), Wayne State University, Detroit, Michigan 48202, United States

<sup>b</sup> International Tomography Center SB RAS, 3A Institutskaya st., Novosibirsk 630090, Russia

<sup>c</sup> Boreskov Institute of Catalysis SB RAS, 5 Acad, Lavrentiev Pr., Novosibirsk 630090, Russia

<sup>d</sup> Department of Pediatrics, Wayne State University, Detroit, Michigan 48202, United States

<sup>e</sup> School of Chemical & Biomolecular Sciences, Materials Technology Center, Southern Illinois University, Carbondale, Illinois 62901, United States

#### Corresponding Authors

E-mail: [nuwandia@wayne.edu](mailto:nuwandia@wayne.edu)

E-mail: [chekmenevlab@gmail.com](mailto:chekmenevlab@gmail.com)

# Table of Contents

1. NMR Spectroscopy Of HP And Thermally Polarized Butane And Propane Gas At 1.4 T .....	S3
2. HP Butane And Propane Gas Proton Signal Enhancement Calculations At 1.4 T .....	S4
3. Reproducibility Of HP Gas $T_1$ Relaxation Experiments At 1 Atm Pressure.....	S5
4. Homogeneous Hydrogenation Of Dissolved 1-Butene, 2-Butene And Propene In $CD_3OD$ At High (1.4 T) And Low (0.0475 T) Magnetic Fields .....	S6
5. HP Butane/Propane NMR Spectroscopy And $T_1$ Relaxation In $CD_3OD$ At 1.4 T.....	S9
6. HP Butane NMR Spectroscopy And $T_s$ Relaxation In $CD_3OD$ At 0.0475 T.....	S10
7. Additional Images Of HP Butane Gas Filled Phantoms .....	S12
8. Additional Ventilation Images Of HP Butane Injected In Rabbit Lungs .....	S20
9. 0.35 T MRI Image Analysis Of HP Gases .....	S21
D) File Storage Format And Architecture.....	S21
ii) Matlab Data Analysis Protocol.....	S21
A) Image_Combination_Analysis.Mat.....	S22
B) Axial_S28_Td_Map.Mat.....	S24
10. Literature Cited In Supporting Information (SI) .....	S29

## 1. NMR spectroscopy of HP and thermally polarized butane and propane gas at 1.4 T

All experiments shown in the **Figure S1** displays were performed at 1.4 T magnetic field via heterogeneous PHIP of butene and propene to produce HP butane and HP propane gas, respectively. **Figure S1** represents an extension of **Figure 2** (main text) with additional information reporting on the chemical conversion (shown by the blue color in displays **c**, **g**, **k**) and thermally polarized reference spectra of the corresponding gases (displays **d**, **h**, **l**). The description of the experiments is provided in the main text. After  $\sim 2$  seconds of continuous flow (6-8 sLm flow rate of produced HP gas), the gas stream was terminated by closing the valves located after the reactor and after the spectrometer (#2 and #3 to create a stopped flow condition) while the data acquisition continued to ensure that HP signal decay was recorded via pseudo-2D NMR acquisition. Examples of such NMR spectra of HP gases are given below in **Figure S1a,e,i**. The recorded spectra were used to calculate the signal enhancements and  $T_1$  relaxation decay (obtained by mono-exponential fitting of the HP signal intensity decay with time; **Figure S1b,f,j**). After HP signal acquisition is completed, a thermally polarized spectrum of the product (butane or propane) gas was also acquired by starting a repeat run of the same acquisition protocol employed for HP acquisition. These thermally polarized spectra allowed to obtain a signal reference (of thermally polarized butane/propane) as shown in **Figure S1d,h,l**), which was then used to calculate signal enhancement values of the HP gas (detailed example calculations are provided further down in the SI). Additionally, thermally polarized spectroscopy (data not shown) was also employed to detect any residual unreacted substrate gas (see the main text for details): **Figure S1c,g,k** shows that nearly 100% chemical conversion of corresponding unsaturated precursors was achieved in all cases as seen by the lack on any olefinic resonances (data not shown). Moreover, for the  $T_1$  pressure dependence studies (**Figure S1c,g,k**), the  $T_1$  values at various pressure were fitted to a straight line because linear  $T_1$  dependence on pressure is anticipated.<sup>1</sup>

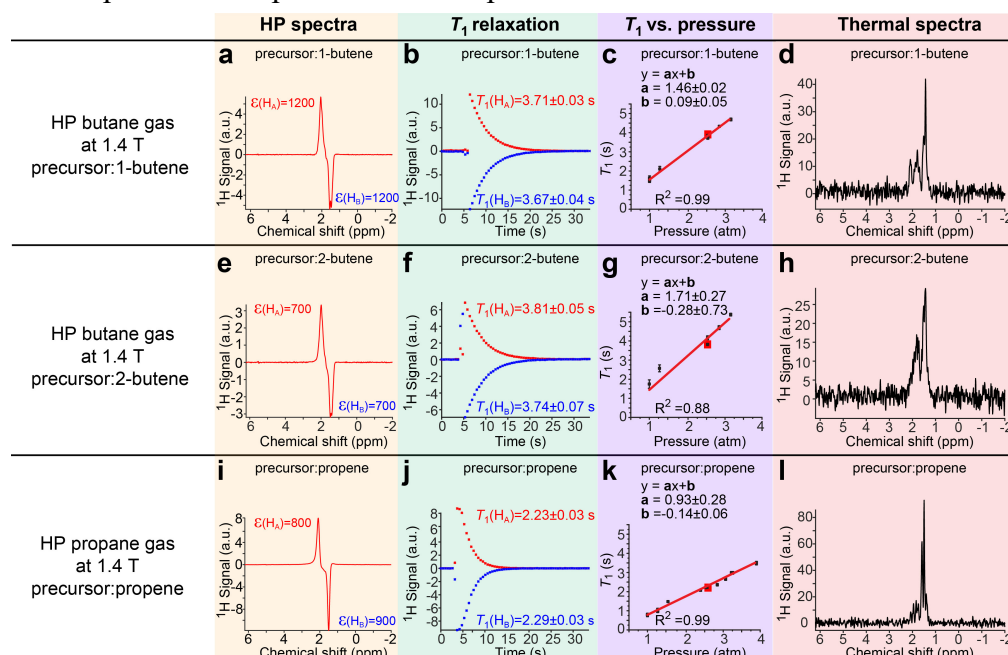


**Figure S1.** NMR studies of HP gas at 1.4 T magnetic field. a) single-scan  $^1\text{H}$  NMR spectrum of HP butane gas produced from PHIP of 1-butene. b)  $T_1$  relaxation plot of HP butane gas produced from 1-butene precursor at the pressure value indicated by red square in display c. c)  $T_1$  dependence of  $H_A$  on pressure (in black) and chemical conversion on pressure (in blue) for HP butane gas produced from 1-butene precursor. d)  $^1\text{H}$  NMR spectrum of thermally polarized butane gas (produced from 1-butene precursor) after the pairwise  $p\text{-H}_2$  addition reaction is completed (64 scans). e)  $^1\text{H}$  NMR spectrum of HP butane gas produced from PHIP of 2-butene precursor. f)  $T_1$  relaxation plot of HP butane gas produced from 2-butene precursor at the pressure value indicated by red square in display g. g)  $T_1$  dependence of  $H_A$  on pressure (in black) and chemical conversion on pressure (in blue) for HP butane gas produced from 2-butene precursor. h)  $^1\text{H}$  NMR spectrum of thermally polarized butane gas (produced from 2-butene precursor) after the pairwise  $p\text{-H}_2$  addition reaction is completed (64 scans). i)  $^1\text{H}$  NMR spectrum of HP propane gas produced from PHIP of propene. j)  $T_1$  relaxation plot of HP propane gas at the pressure value indicated by red square in display k. k)  $T_1$  dependence of  $H_A$  on pressure (in black) and chemical conversion on pressure (in blue) for HP propane gas. l)  $^1\text{H}$  NMR spectrum of thermally polarized propane gas after the pairwise  $p\text{-H}_2$  addition reaction is completed (64 scans). Different color codes for vertical columns are provided here as a guide the eye to distinguish HP spectra (light yellow color),  $T_1$  relaxation (light green color),  $T_1$  dependence of  $H_A$  (light purple color) and corresponding thermal spectra (light brown color).

## 2. HP butane and propane gas proton signal enhancement calculations at 1.4 T

Here, we discuss automated data analysis protocol using MATLAB (R2021a). All the data recorded using Nanalysis (1.4 T Nanalysis NMR Pro 60, New-Zealand) were analyzed using the following script. Corresponding figures created using this MATLAB script are presented in **Figures 2a,b,d,e,g,h** and **Figure S1a,b,d,e,f,h,i,j,l**.

Quotation marks ('Reference Data') are used to show directories and variable names. Comments and operation (preceded with “%” symbol), are shown in the script as a guide to understanding of the code structure. *i.e.*, % this is a comment.

The HP butane/propane signal data (64 repeat scans as described in the main text experimental section under **Fast pseudo 2D acquisition pulse sequence**) are previously stored in a folder named as “HP data” and the thermally polarized butane signal reference data are stored in a folder named as “Reference data”. According to the pseudo-acquisition method, 64 repeat scans are recorded for the HP state for a single experimental run in an accumulated data acquisition fashion, *i.e.*, all 64 spectra are combined, and experimental data is also stored as a sum of 64, 63, 62, ... 1, spectra, respectively. Therefore, we perform a de-accumulation of data prior to calculating their integrated intensities (see the MATLAB script provided in a separate SI). The example of the pseudo-2D data and MATLAB code is provided in a separate SI zip file.

First, we clean the workspace to make sure it is not filled with unwanted commands/functions from previous runs. Line broadening, phase correction and baseline correction are performed before the data integration begins. The script is written in such a way that 64 HP signal plots and their corresponding thermal spectrum are created and exported as pdfs with a csv file that contains the signal intensities and signal enhancement values. For relaxation data analysis, a build-up curve is created for all the 64 HP signal data files and a separate decay curve is fitted for selected integrated signal intensities obtained from a frequency range of interest (the frequency is specified by “bound 7” and “bound 8” in the code) using an exponential decay function.

HP butane/propane gas signal enhancements were calculated using the ratio of the signal intensity of the hyperpolarized proton and the signal intensity of the thermally polarized protons of butane gas after hydrogenation using the equations Eq. S1-S2 below.

$$EHa(k) = (SHa(k)/Stherm\_avg) * 10 \quad (\text{Eq. S1})$$

$$EHb(k) = (SHb(k)/Stherm\_avg) * 10 \quad (\text{Eq. S2})$$

$EHa(k)$  and  $(EHb(k))$  are the signal enhancement values of the protons of interest ( $H_A$  or  $H_B$ ) and  $SHa(k)$  is the integrated signal intensity of the HP proton of interest, and  $Stherm\_avg$  is the integrated signal intensity of the thermally polarized molecule (employed as a signal reference with known polarization). Since thermally polarized propane and butane have total of 8 protons and 10 protons respectively, the proton ratio of 10 (equations S1 and S2) was used for butane gas (this comes from the proton ratio of the thermal spectrum (originating from 10 protons) and the HP spectrum for HP butane (originating from 1 proton for each  $H_A$  and  $H_B$  lines), and therefore gives  $10/1 = 10$  for butane gas calculations. This value becomes 8 for propane gas enhancement calculations because proton ratio of thermally polarized propane to HP propane becomes  $= 8/1 = 8$  for propane. The MATLAB script was used to calculate signal enhancements, fitting of the decay data as well as plotting the spectra and relaxation plots. The complete MATLAB script of automated data analysis is given in a separate SI zip file.

### 3. Reproducibility of HP gas $T_1$ relaxation experiments at 1 atm pressure

#### Reproducibility of $T_1$ measurements at 1 atm

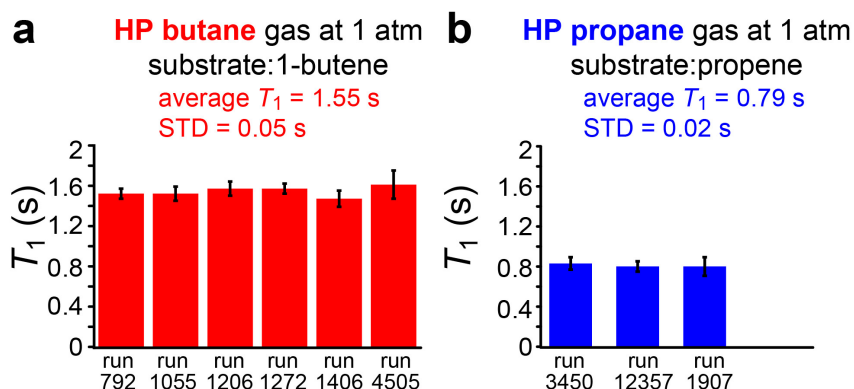


**Figure S2.** a) Reproducibility plot of  $T_1$  data collected for HP butane gas (produced from 1-butene precursor) at atmospheric (1 bar) gas pressure. This display shows shot-to-shot reproducibility of the experimental technique used in obtaining  $T_1$  decay of HP gases (using 6 individual runs at 1 bar/atm total gas pressure of HP butane gas, **Table S1**). b) The shot-to-shot reproducibility plot of  $T_1$  data collected for HP propane gas at atmospheric (1 bar/1 atm) gas pressure, **Table S1**. The standard deviation (STD)  $T_1$  values are also reported for each HP gas.

**Table S1.** Pressure dependence data of  $T_1$  of  $H_A$  site and  $H_B$  site for HP butane gas (produced from two precursor molecules: 1-butene and 2-butene) and HP propane gas (produced from propene precursor). The data sets marked with asterisk (\*) are presented in **Figure 2**.

Pressure (atm)	Butane from 1-butene		Butane from 2-butene		Propane from propene		Butane from 1-butene		Butane from 2-butene		Propane from propene	
	$T_1$ $H_A$ (s)	$T_1$ $H_A$ error bar (s)	$T_1$ $H_A$ (s)	$T_1$ $H_A$ error bar (s)	$T_1$ $H_A$ (s)	$T_1$ $H_A$ error bar (s)	$T_1$ $H_B$ (s)	$T_1$ $H_B$ error bar (s)	$T_1$ $H_B$ (s)	$T_1$ $H_B$ error bar (s)	$T_1$ $H_B$ (s)	$T_1$ $H_B$ error bar (s)
1.00	1.53 (run 792)	0.05	1.74 (run 1848)	0.22	0.81 (run 3450)	0.06	1.42	0.10	1.33	0.31	0.73	0.06
1.00	1.53 (run 1055)	0.07	-	-	0.78 (run 12357)	0.05	1.41	0.12	-	-	0.79	0.03
1.00	1.58 (run 1206)	0.07	-	-	0.78 (run 1907)	0.09	1.50	0.13	-	-	0.76	0.11
1.00	1.58 (run 1272)	0.05	-	-	-	-	1.49	0.09	-	-	-	-
1.00	1.48 (run 1406)	0.08	-	-	-	-	1.44	0.07	-	-	-	-
1.00	1.62 (run 4505)	0.12	-	-	-	-	1.62	0.10	-	-	-	-
1.28	2.10 (run 0002)	0.14	2.56 (run 1716)	0.18	0.96 (run 1775)	0.04	1.71	0.21	2.14	0.16	0.98	0.06
1.28	-	-	-	-	1.03 (run 12225)	0.09	-	-	-	-	0.92	0.12
1.28	-	-	-	-	1.01 (run 3318)	0.04	-	-	-	-	0.97	0.06
1.56	-	-	-	-	1.48 (run 11961)	0.1*	-	-	-	-	1.43	0.06
2.39	-	-	-	-	2.07 (run 12093)	0.05	-	-	-	-	1.98	0.10
2.53	3.71 (run 1923)*	0.03*	4.16 (run 1584)	0.10	2.23 (run 1086)*	0.03*	3.67*	0.04*	3.63	0.21	2.29*	0.03*
2.53	3.84 (run 0662)	0.07	3.81 (run 0397)*	0.05*	-	-	3.75	0.13	3.74*	0.07*	-	-
2.56	-	-	-	-	2.22 (run 3186)	0.05	3.7	0.10	3.9	0.20	2.32	0.08
2.84	4.33 (run 1086)	0.05	4.69 (run 1451)	0.10	2.36 (run 3054)	0.06	4.07	0.11	4.13	0.15	2.48	0.09
3.07	-	-	-	-	2.65 (run 12634)	0.06	-	-	-	-	2.55	0.12
3.15	4.69 (run 0398)	0.07	4.55	0.15	-	-	5.37	0.07	4.53	0.22	-	-
3.22	-	-	-	-	2.98 (run 2922)	0.07	-	-	-	-	3.10	0.11
3.26	-	-	-	-	2.98 (run 12502)	0.07	-	-	-	-	3.01	0.12
3.90	-	-	-	-	3.49 (run 11567)	0.09	-	-	-	-	3.40	0.14

**Table S2.** Pressure dependence data of  $T_s$  for HP butane gas (produced from two precursor molecules: 1-butene and 2-butene) and HP propane gas (produced from propene precursor). The data sets marked with asterisk (\*) are presented in **Figure 3**.

Pressure (atm)	Butane from 1-butene		Butane from 2-butene		Propane from propene	
	$T_s$ (s)	$T_s$ error bar (s)	$T_s$ (s)	$T_s$ error bar (s)	$T_s$ (s)	$T_s$ error bar (s)
1.00			2.80 (run 21)	0.01		
1.00			3.20 (run 22)	0.18		
1.01	3.57 (run 11)	0.03	3.15 (run 09)	0.05	2.54 (run 09)	0.03
1.01	3.81 (run 15)	0.03	2.87 (run 10)	0.05	2.42 (run 10)	0.03
1.12					3.00 (run 06)	0.01
1.12					3.04 (run 07)	0.01
1.16	4.22 (run 09)	0.01				
1.18	4.12 (run 14)	0.02				
1.20	4.35 (run 08)	0.01				
1.22			3.14 (run 07)	0.03	2.45 (run 08)	0.01
1.23			3.60 (run 19)	0.04		
1.56	4.62 (run 06)	0.02				
1.57					3.64 (run 05)	0.02
1.60			3.81 (run 17)	0.03		
1.62			3.86 (run 05)	0.02		
1.62			3.95 (run 06)	0.02		
1.90	5.78 (run 04)*	0.01*	4.74 (run 15)*	0.01*		
1.90	5.32 (run 05)	0.01	4.77 (run 16)	0.02		
1.90	5.72 (run 03)	0.02				
1.94			4.65 (run 03)	0.01	3.74 (run 03)*	0.01*
1.94			4.53 (run 04)	0.02	3.72 (run 04)	0.01
2.49					4.68 (run 01)	0.01
2.53					4.36 (run 02)	0.01
2.61	6.46 (run 02)	0.01				
2.63	6.37 (run 10)	0.01				

#### 4. Homogeneous hydrogenation of dissolved 1-butene, 2-butene and propene in CD<sub>3</sub>OD at high (1.4 T) and low (0.0475 T) magnetic fields.

All the experiments were performed in CD<sub>3</sub>OD solvent. Regular-wall 5-mm NMR tubes were prepared with a Teflon jacket (1/4-inch OD, 3/16-in ID tubing, ~3-inch long) attachment connected to the top of NMR tube. 0.6 mL of CD<sub>3</sub>OD containing 4 mM of Rh[(COD)(dppb)]BF<sub>4</sub> catalyst (COD = 1,5-cyclooctadiene, dppb = 1,4-bis(diphenylphosphino)butane) (Sigma-Aldrich, P/N 341134) was pipetted into the NMR tube first. The catalyst solution was then saturated with the substrate gas by slowly bubbling the substrate into the NMR tube for 1 minute and then capping the NMR tube. This sample was then connected to the push-to-connect “Y” fitting. This fitting has 1/4” end connected to the NMR tube, and the other two ends are employed as the p-H<sub>2</sub> gas inlet and exit path for used p-H<sub>2</sub> gas venting, respectively. The inlet line (1/8” OD Teflon tubing, 1/16” ID) is additionally equipped with the Teflon catheter (1/16-inch OD, 1/32-inch ID) that is inserted in the inlet 1/16” ID tubing and runs all the way to the bottom of the NMR tube, **Figure S3**. The NMR tube was then connected to rest of the setup as shown in **Figure S3**, providing access to p-H<sub>2</sub> source through the gas inlet tube.<sup>2</sup> Once connected to the p-H<sub>2</sub> source, the tube was pressurized to 7 atm of p-H<sub>2</sub> overpressure using the bypass valve (the open position prevents p-H<sub>2</sub> gas bubbling through the sample). The pressurized sample was then heated for 30 s at 60 °C. Next, it was bubbled with p-H<sub>2</sub> for 15 s at the Earth’s magnetic field. Next, bypass valve was opened (to stop p-H<sub>2</sub> bubbling), and the

sample was depressurized by removing a relief valve. The push-to-connect was disconnected, and the catheter was removed from the sample tube. Finally, the sample was quickly transferred to the 1.4 T NMR spectrometer for detection, **Figure S3**, resulting in the appearance of ALTADENA<sup>3</sup> spectral patterns.

Once the sample was inserted in the 1.4 T spectrometer (Magritek, SpinSolve Carbon), NMR spectra (shown in **Figures S4a,c,e**) were acquired (using 9° RF excitation pulse) in the pseudo-2D mode every 10 seconds, **Scheme S1a**. The signal decay was estimated by fitting the HP signal intensity data with time onto a mono-exponential decay curve, **Figures S4b,d,f**. In case of NMR studies at 0.0475 T, the catheter was kept inside the NMR tube. Once the sample was inserted in the 0.0475 T spectrometer, the data was acquired in a pseudo-2D fashion (every 5 seconds) using the protocol shown in **Scheme S1b**. The singlet to triple conversion was achieved using partial SLIC pulses of 0.3 seconds long. In case if the SLIC pulse was not applied, no signal was detected (data not shown). The mono-exponential fitting of the recorded signal decay data (using the integrated intensity of the HP peak at different time intervals) was done using automated fitting script via MATLAB.

### experimental setup for homogeneous hydrogenation

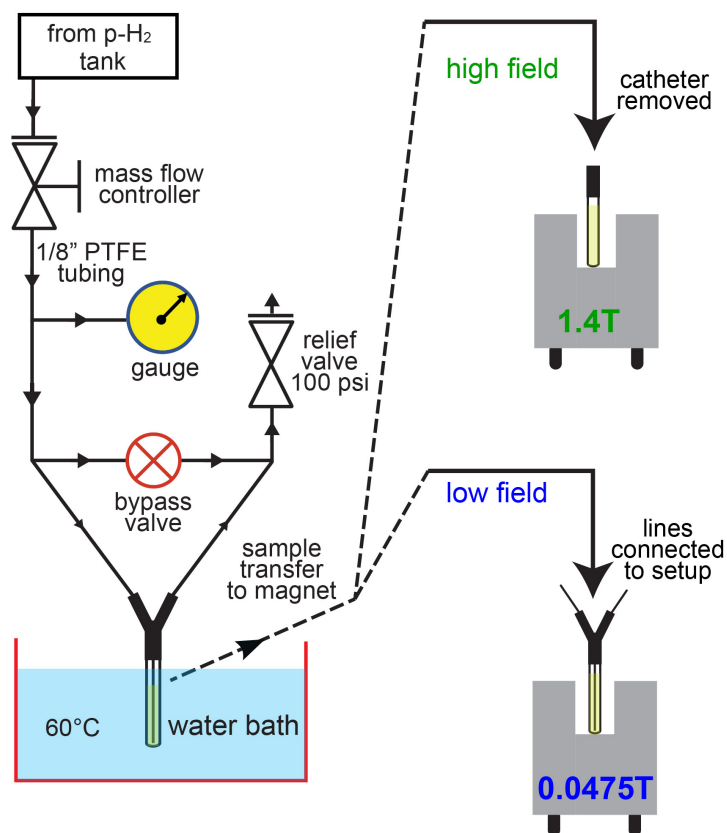
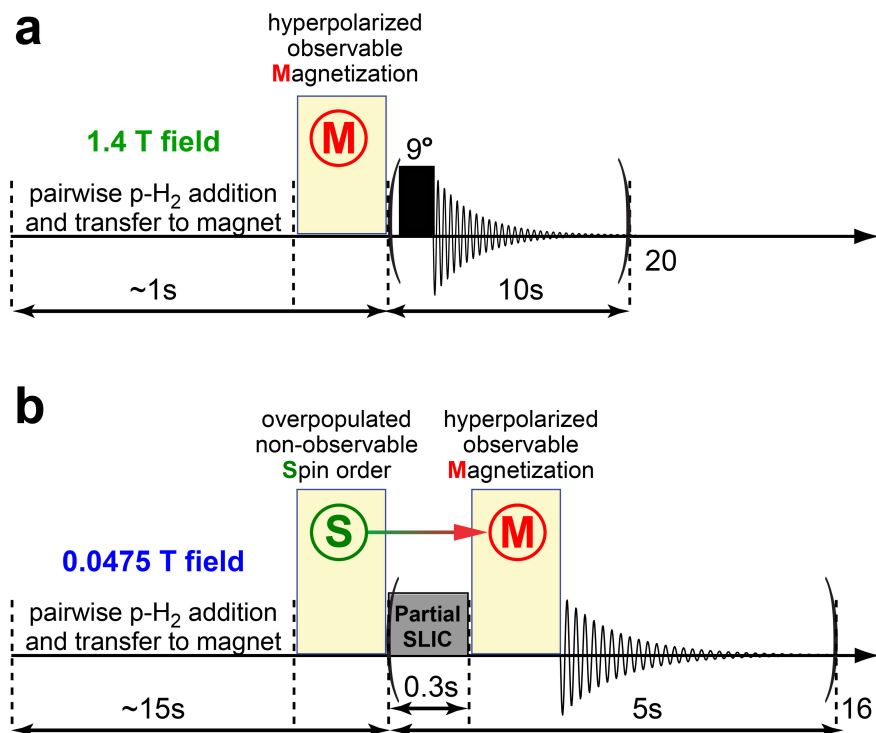


**Figure S3.** Schematic of NMR studies of homogeneous pairwise p-H<sub>2</sub> addition to dissolved butene and propene in CD<sub>3</sub>OD solvent at high (1.4 T) and low (0.0475 T) magnetic fields.

**Scheme S1.** Schematic diagram of the pulse sequences used for the detection of HP gas (butane or propane) dissolved in CD<sub>3</sub>OD in the weakly coupled regime (*i.e.*, high field of 1.4 T) and the strongly coupled regime (*i.e.*, low field of 0.0475 T). a) The sequence applied for signal detection at 1.4 T field starts with pairwise p-H<sub>2</sub> addition to the to-be-hydrogenated substrate in the Earth's magnetic field; next, the sample is transferred to the detection field of 1.4 T; finally, the sequence ends with application of a series of back-to-back scans (total of 20): each scan starts with 9° small-angle excitation RF pulse followed by FID signal acquisition. The data is acquired in pseudo-2D fashion with the time duration of each repeat run of approximately 10 seconds. b) The pulse sequence for singlet to triplet state conversion at 0.0475 T using SLIC; this sequence starts with pairwise p-H<sub>2</sub> addition to the to-be-hydrogenated substrate in the Earth's magnetic field (by bubbling p-H<sub>2</sub> gas into the substrate catalyst solution for 15 s) followed by the sample transfer into the magnet. Then, singlet-to-triplet magnetization conversion is achieved by applying a SLIC pulse followed by FID signal acquisition for 16 individual spectral runs. Each spectral acquisition employs 0.3 s duration SLIC pulse and each signal is acquired every 5 seconds.





## 5. HP butane/propane NMR spectroscopy and $T_1$ relaxation in $\text{CD}_3\text{OD}$ at 1.4 T

**NMR spectroscopy,  $T_1$  and  $T_S$  relaxation dynamics of HP propane and butane dissolved in  $\text{CD}_3\text{OD}$  at 1.4 T and 0.0475 T.** We have also performed relaxation dynamics studies of HP butane and HP propane following dissolution in  $\text{CD}_3\text{OD}$  (SI). The  $T_1$  values measured at 1.4 T for HP butane were effectively the same (within experimental error) for the samples employing 1-butene (e.g.,  $T_1(\text{H}_A)=31.7\pm 0.8$  s) and 2-butene ( $T_1(\text{H}_A)=33.3\pm 1.1$  s), echoing the results in the gas phase. Of note, HP propane exhibited longer  $T_1(\text{H}_A)$  of  $42.5\pm 2.5$  s, **Figure S4**—this is not unexpected since in liquid phase the relaxation is governed by dipolar interactions rather than the spin-rotation mechanism. Relaxation dynamics of dissolved HP butane and HP propane at 0.0475 T also overall supported the observations and conclusion made for the gas phase studies above: HP butane produced from 1-butene exhibited  $T_S$  of  $19.5\pm 0.7$  s, whereas HP butane produced from 2-butene shows  $T_S$  of  $16.9\pm 0.6$  s (of note, the comparative  $T_S$  value for HP propane was  $15.7\pm 0.7$  s), **Figure S5**. This observation is important as it supports the conclusions made for  $T_S$  in the gas phase: different LLSS are being created in each case, and LLSS created from 1-butene PHIP precursor generally has longer lifetimes.

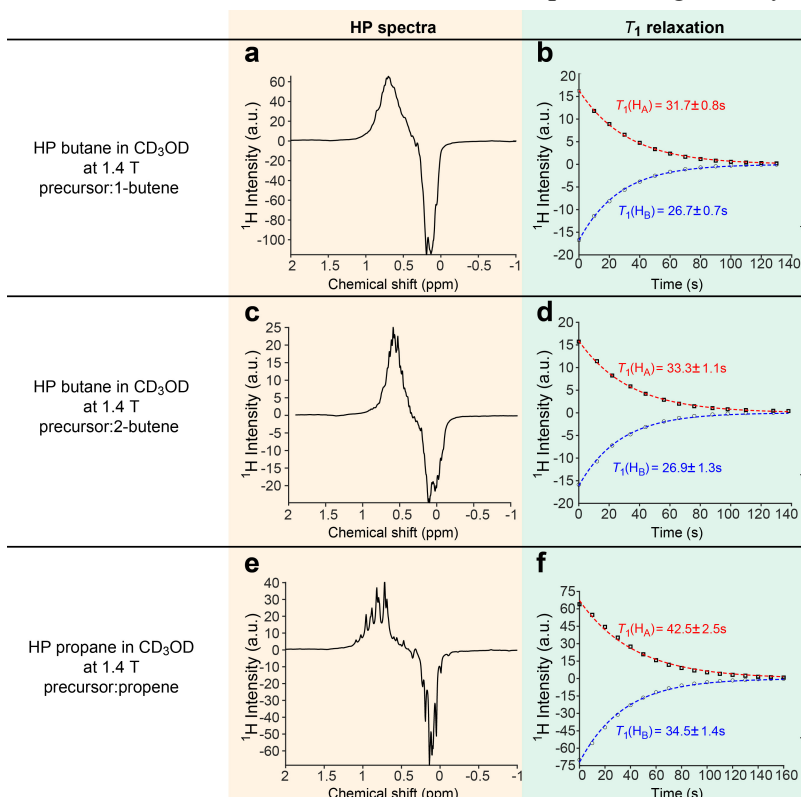


**Figure S4.** 1.4 T NMR spectroscopy and  $T_1$  relaxation dynamics of HP butane and HP propane dissolved in  $\text{CD}_3\text{OD}$  produced via homogeneous p- $\text{H}_2$  pairwise addition. a)  $^1\text{H}$  NMR spectrum of HP butane dissolved in  $\text{CD}_3\text{OD}$  produced from 1-butene substrate. b)  $T_1$  relaxation decay plot of HP butane dissolved in  $\text{CD}_3\text{OD}$ . c)  $^1\text{H}$  NMR spectrum of HP butane dissolved in  $\text{CD}_3\text{OD}$  produced from 2-butene substrate. d)  $T_1$  relaxation decay plot of HP butane dissolved in  $\text{CD}_3\text{OD}$ . e)  $^1\text{H}$  NMR spectrum of HP propane dissolved in  $\text{CD}_3\text{OD}$  produced from propene substrate. f)  $T_1$  relaxation decay plot of HP propane dissolved in  $\text{CD}_3\text{OD}$ . The HP spectra are highlighted using light yellow color and  $T_1$  relaxation plots are highlighted using a light green color.

Spectroscopy and relaxation dynamics of the dissolved HP butane and propane dissolved in  $\text{CD}_3\text{OD}$  employed the experimental setup shown in **Figure S3**. **Figure S4a,c,e** shows NMR spectra of HP butane and propane with typical ALTADENA type signal in the weakly coupled regime with positively and negatively aligned proton signals. The corresponding ( $\text{H}_A$  or  $\text{H}_B$ )  $T_1$  values of HP butane (produced from both 1-butene and 2-butene) significantly differ from those of HP propane (in the dissolved phase). On the other hand, the  $T_1$  values of HP butane produced from either 1-butene or 2-butene are essentially the same, i.e.,  $31.7\pm 0.8$  s vs.  $33.3\pm 1.1$  s for  $\text{H}_A$ , and  $26.9\pm 1.3$  s vs.  $26.7\pm 0.7$  s for  $\text{H}_B$ , **Figure S4b,d,f**. This is not surprising as at the high field (1.4 T) the long-lived spin states (LLSS) do not exist, and each site ( $\text{H}_A$  or  $\text{H}_B$ ) effectively decays at its own relaxation rate. Additionally, the substantially lower  $T_1$  values of gas-phase HP products vs. that in  $\text{CD}_3\text{OD}$  is rationalized by a different (and generally more efficient) relaxation mechanism occur in the gas phase compared to that in the liquid phase.

## 6. HP butane NMR spectroscopy and $T_S$ relaxation in $CD_3OD$ at 0.0475 T

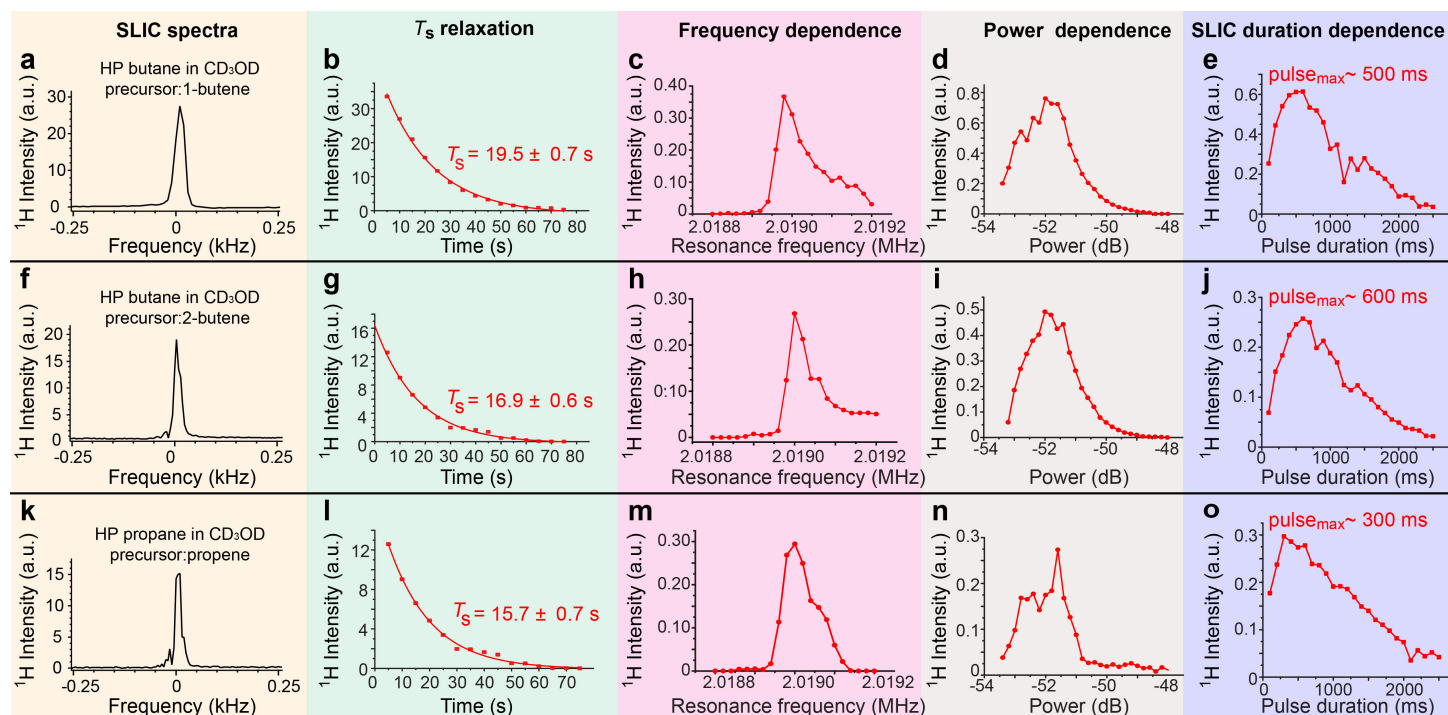


**Figure S5.** 0.0475 T NMR spectroscopy and  $T_1$  relaxation dynamics of HP butane and HP propane dissolved in  $CD_3OD$  produced via homogeneous  $p-H_2$  pairwise addition. a) NMR spectrum obtained after applying SLIC pulse (using 0.3-s SLIC pulse duration, -52 dB power, 2.0190 MHz resonance frequency) of HP butane produced via pairwise addition of  $p-H_2$  to dissolved 1-butene precursor. b) Effective  $T_S$  relaxation decay with mono-exponential fitting curve for HP butane produced via pairwise  $p-H_2$  addition to dissolved 1-butene precursor (each data point was acquired using the parameters used for data acquisition shown in display a). c) NMR signal of HP butane (produced via pairwise  $p-H_2$  addition to dissolved 1-butene) dependence on resonance frequency of the applied SLIC pulse (using 0.3-s SLIC pulse duration at -52 dB power). d) HP butane (produced via pairwise  $p-H_2$  addition to dissolved 1-butene precursor) signal dependence on the SLIC pulse power in the units of dB power setting (using 0.3-s SLIC pulse duration and 2.0190 MHz resonance frequency). e) The dependence of NMR signal of HP butane (produced via pairwise  $p-H_2$  addition to dissolved 1-butene precursor) on the duration of SLIC pulse (using -52 dB SLIC power setting and 2.0190 MHz resonance frequency). f) NMR spectrum obtained after applying SLIC pulse (using 0.3-s SLIC pulse duration, -52 dB power, 2.0190 MHz resonance frequency) of HP butane produced via pairwise addition of  $p-H_2$  to dissolved 2-butene precursor. g) Effective  $T_S$  relaxation decay with mono-exponential fitting curve for HP butane produced via pairwise  $p-H_2$  addition to dissolved 2-butene precursor (each data point was acquired using the parameters used for data acquisition shown in display f). h) NMR signal of HP butane (produced via pairwise  $p-H_2$  addition to dissolved 2-butene) dependence on resonance frequency of the applied SLIC pulse (using 0.3-s SLIC pulse duration at -52 dB power). i) HP butane (produced via pairwise  $p-H_2$  addition to dissolved 2-butene precursor) signal dependence on the SLIC pulse power in the units of dB power setting (using 0.3-s SLIC pulse duration and 2.0190 MHz resonance frequency). j) The dependence of NMR signal of HP butane (produced via pairwise  $p-H_2$  addition to dissolved 2-butene precursor) on the duration of SLIC pulse (using -52 dB SLIC power setting and 2.0190 MHz resonance frequency). k) NMR spectrum obtained after applying SLIC pulse (using 0.3-s SLIC pulse duration, -52 dB power, 2.0190 MHz resonance frequency) of HP propane produced via pairwise addition of  $p-H_2$  to dissolved propene precursor. l) Effective  $T_S$  relaxation decay with mono-exponential fitting curve for HP propane produced via pairwise  $p-H_2$  addition to dissolved propene precursor (each data point was acquired using the parameters used for data acquisition shown in display k). m) NMR signal of HP propane (produced via pairwise  $p-H_2$  addition to dissolved propene) dependence on resonance frequency of the applied SLIC pulse (using 0.3-s SLIC pulse duration at -52 dB power). n) HP propane (produced via pairwise  $p-H_2$  addition to dissolved propene precursor) signal dependence on the SLIC pulse power in the units of dB power setting (using 0.3-s SLIC pulse duration and 2.0190 MHz resonance frequency). o) The dependence of NMR signal of HP propane (produced via pairwise  $p-H_2$  addition to dissolved propene precursor) on the duration of SLIC pulse (using -52 dB SLIC power setting and 2.0190 MHz resonance frequency). All pseudo-2D optimization experiments, e.g., the trends shown in displays b, c, d, e, employed one HP sample to perform an entire 2D acquisition. The HP spectra are highlighted using light yellow color,  $T_S$  relaxation plots are highlighted using a light green color, resonance frequency optimization plots are highlighted with light magenta color, the power optimization plots are highlighted with grey color, and SLIC pulse duration plots are highlighted with blue color.

In addition to homogeneous hydrogenation in the weakly coupled regime (studies performed at 1.4 T), we also studied homogeneous p-H<sub>2</sub> pairwise addition to 1-butene, 2-butene and propene precursors in the strongly coupled magnetic field regime (*i.e.*, at 0.0475 T) using SLIC pulse (to transform LLSS into observable magnetization) to investigate the feasibility of creating LLSS in the low magnetic field and the LLSS lifetime governed by  $T_S$ . If no SLIC was applied, no NMR signal was obtained due to cancellation of H<sub>A</sub> and H<sub>B</sub> resonances with opposite phases. Applying SLIC pulse to HP butane or propane (created under ALTADENA conditions) in CD<sub>3</sub>OD visualized the creation of z-magnetization (**Figure S5a,f,k**) in line with previous SLIC studies on HP liquid propane.<sup>1</sup> These studies shown in **Figure S5** reveal that relaxation dynamics of LLSS created in HP butanes from 1-butene and 2-butene are different. HP propane exhibits  $T_S$  value of  $15.7 \pm 0.7$  s; HP butane (produced from 1-butene) exhibits  $T_S$   $19.5 \pm 0.7$  s, and HP butane (produced from 2-butene) has  $T_S$  of  $16.9 \pm 0.6$  s. The somewhat unexpected finding that  $T_S$  values for dissolved HP butane are different when different precursors were employed is rationalized by the potentially different spin states that are being overpopulated after pairwise p-H<sub>2</sub> addition. This finding echoes the gas phase  $T_S$  results (see main text), also demonstrating that  $T_S$  of gas-phase butane is longer when 1-butene precursor is employed for PHIP. Moreover,  $T_S$  values of HP butanes were also longer than that of HP propane, once again, echoing the corresponding trend for gas-phase  $T_S$  values discussed in the main text. One should not be directly comparing the effective  $T_S$  values and  $T_1$  values in the liquid state because  $T_S$  was measured by applying SLIC pulses for subsequent measurement on the same sample, thus, the sample additionally experiences depolarization due to SLIC irradiation, which was not taken into account. The studies of experimental parameters optimization for SLIC pulse resonance frequency, power and duration revealed overall the same trends for HP butane and propane dissolved in CD<sub>3</sub>OD, **Figure S5**. The optimized experimental SLIC parameters (**Figure S5**) were employed for  $T_S$  relaxation studies of the gas-phase HP butanes and propane (see the main text).

## 7. Additional images of HP butane gas filled phantoms

### a) Axial S32 HP butane MRI scanning (axial butane reproducibility run 1)

We have run the reproducibility study of HP butane axial 2D GRE MRI described in the main text. The images show the temporal evolution of HP butane, with intensities mapped with color bar. A total of 16 scan were recorded; each scan acquisition time was 0.97 s. Continuation of HP butane gas flow was stopped at scan #4 (flowing artifacts are seen in **Figure S6a**, scan #3). Therefore, HP state could only start to decay at scan #4 and after. As a result, the effective HP signal decay (with mono-exponential  $T_d$  constant reflecting HP signal decay due to compounding effects of nuclear spin relaxation and the effect of the applied excitation RF pulses) was measured using the following difference images intensity: (scan #4 – scan #16), (scan #5 – scan #16), (scan #6 – scan #16), (scan #7 – scan #16), (scan #8 – scan #16) and, (scan #9 – scan #16). Effective  $T_d$  was found to be  $1.15 \pm 0.19$  seconds, **Figure S6c**.

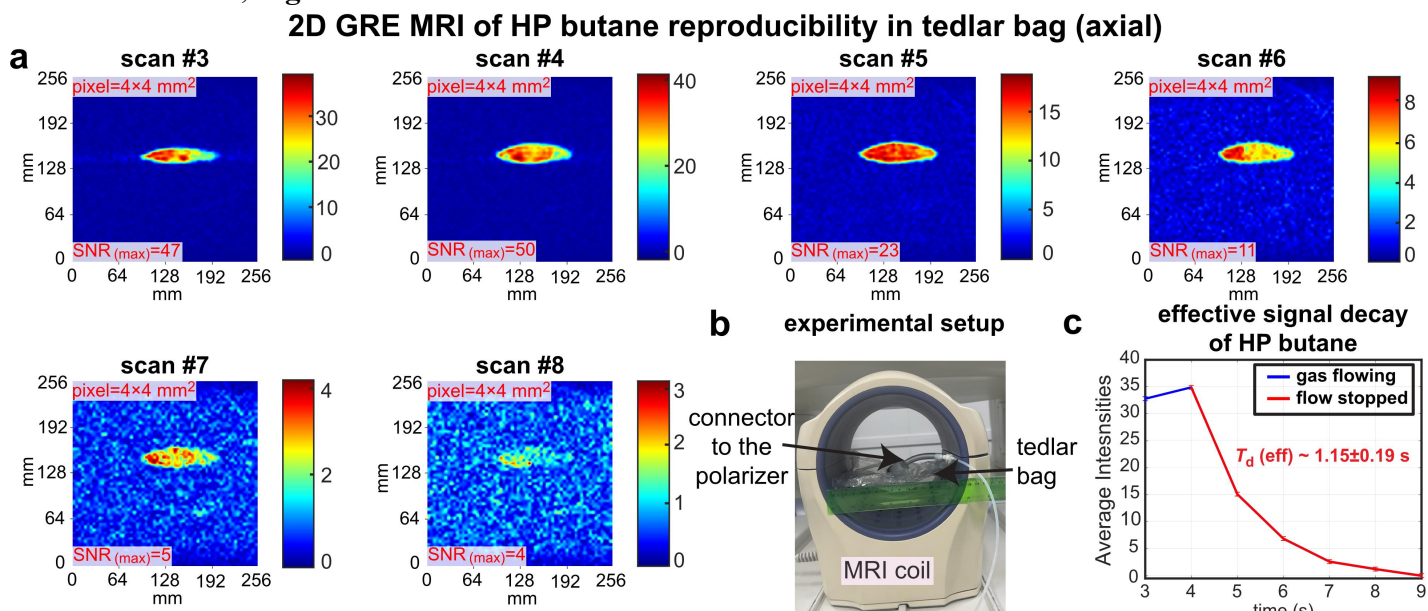


**Figure S6.** Sub-second slice-selective 2D GRE axial images of HP butane gas injected in a one-liter Tedlar bag and recorded with  $64 \times 64$  imaging matrix (converted to  $256 \times 256$  in post image processing) covering a  $256 \times 256$  mm<sup>2</sup> FOV, 50-mm slice thickness, and 30° slice-selective RF pulse. a) Intensity color-mapped images, tracking the changing dynamics of HP butane gas before, during and after HP gas injection inside the Tedlar bag. To quantify the image quality,  $SNR_{(MAX)}$  values were calculated by taking the ratio of the highest intensity matrix element from a  $3 \times 3$  matrix in highest intensity of the inflated region and a random RMS noise region (examples of such selection regions are shown in **Figure 5a,b** of the main text). b) An annotated closeup photograph provides insight to the experimental configuration, highlighting the knee MRI coil, connection to the polarizer and the Tedlar bag, with a ruler for scale. c) Averaged intensities of HP butane of the selected  $3 \times 3$  matrix elements plotted over time: each second corresponds to one image acquisition. Averaged intensities are calculated from  $3 \times 3$  matrix elements from the highest intensity region before the gas flow was stopped (time point 3 s) and averages are taken from exactly the same position during the HP signal decay (time points 4-9 s). The last 5 data points during the HP gas relaxation (when the HP gas flow was definitely stopped) were used to determine the effective  $T_d$  decay constant of  $1.15 \pm 0.19$  s using the model of mono-exponential decay.

## b) Axial S28 HP butane MRI scanning (axial butane reproducibility run 2)

We have run the repeat of reproducibility study of HP butane axial 2D GRE MRI described in the main text and SI. The images depict the temporal evolution of HP butane, with intensities mapped with color bar. A total of 16 scans were recorded, each scan acquisition time was 0.97 s. Continuation of HP butane gas flow was stopped at scan #4. Therefore, HP state could only start to decay at scan #4 and after. As a result, the effective HP signal decay (with mono-exponential  $T_d$  constant reflecting HP signal decay due to compounding effects of nuclear spin relaxation and the effect of the applied excitation RF pulses) was measured using the following difference images intensity: (scan #4 – scan #16), (scan #5 – scan #16), (scan #6 – scan #16), (scan #7 – scan #16), (scan #8 – scan #16) and, (scan #9 – scan #16). Effective  $T_d$  was found to be  $1.04 \pm 0.24$  seconds.

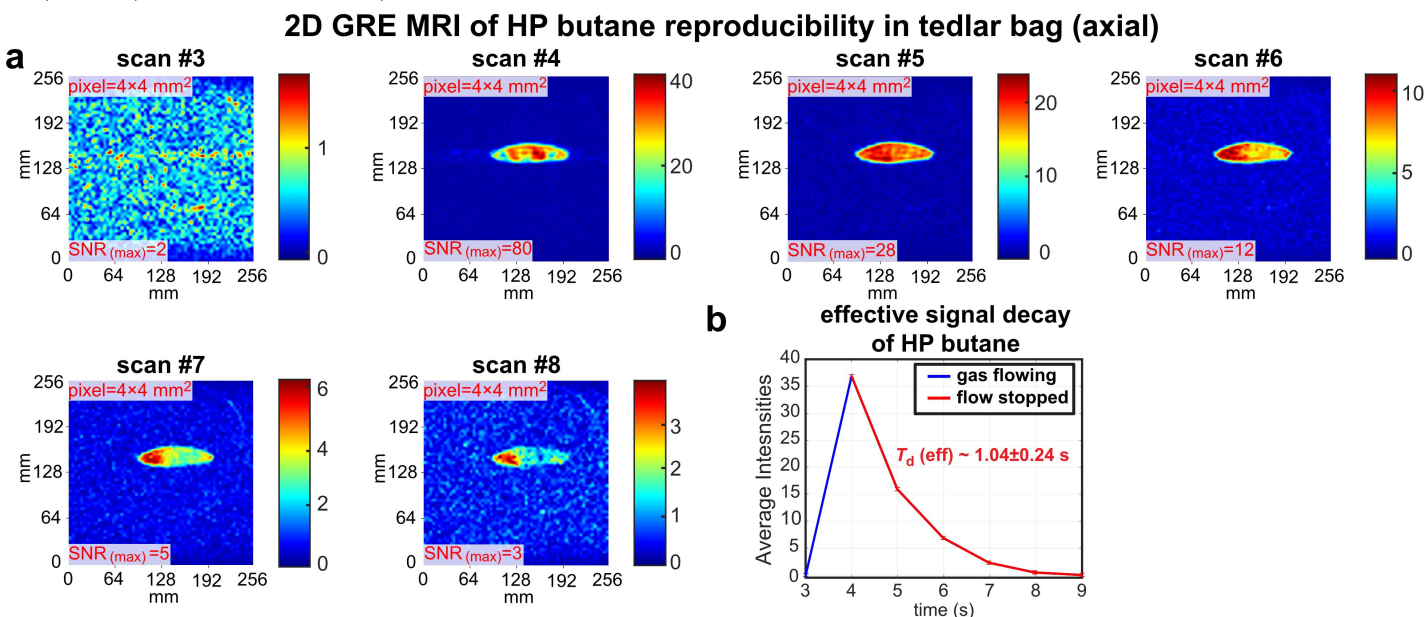


**Figure S7.** Sub-second slice-selective 2D GRE axial images of HP butane gas injected in a one-liter Tedlar bag and recorded with  $64 \times 64$  imaging matrix (converted to  $256 \times 256$  in post image processing) covering a  $256 \times 256$  mm<sup>2</sup> FOV, 50-mm slice thickness, and  $30^\circ$  slice-selective RF pulse. a) Intensity color-mapped images, tracking the changing dynamics of HP butane gas before, during and after HP gas injection inside the Tedlar bag. To quantify the image quality,  $SNR_{(MAX)}$  values were calculated by taking the ratio of the highest intensity matrix element from a  $3 \times 3$  matrix in highest intensity of the inflated region and a random RMS noise region (examples of such selection regions are shown in **Figure 5a,b** of the main text). b) Averaged intensities are calculated from  $3 \times 3$  matrix elements from the highest intensity region before the gas flow was stopped (time point 3 s) and averages are taken from exactly the same position during the HP signal decay (time points 4-9 s). The last 5 data points during the HP gas relaxation (when the HP gas flow was definitely stopped) were used to determine the effective  $T_d$  signal decay constant of  $1.04 \pm 0.24$  seconds using the model of mono-exponential decay.

### c) Axial S12 HP propane MRI scanning (axial propane reproducibility run 1)

We have also performed the reproducibility study of HP propane axial 2D GRE MRI described in the main text. The images depicting the temporal evolution of HP propane signal similarly to the HP butane reproducibility studies described above. A total 16 scans were recorded, each slice represents  $\sim 0.97$  sec. Continuation of HP propane gas flow was definitely stopped at scan #4. Therefore, HP state signal could only decay at scan #4 and after. As a result, the  $T_d$  was measured using the following difference images intensity: (scan #4 – scan #16), (scan #5 – scan #16), (scan #6 – scan #16), (scan #7 – scan #16), (scan #8 – scan #16) and, (scan #9 – scan #16). Effective  $T_d$  was found to be  $0.99 \pm 0.13$  seconds.

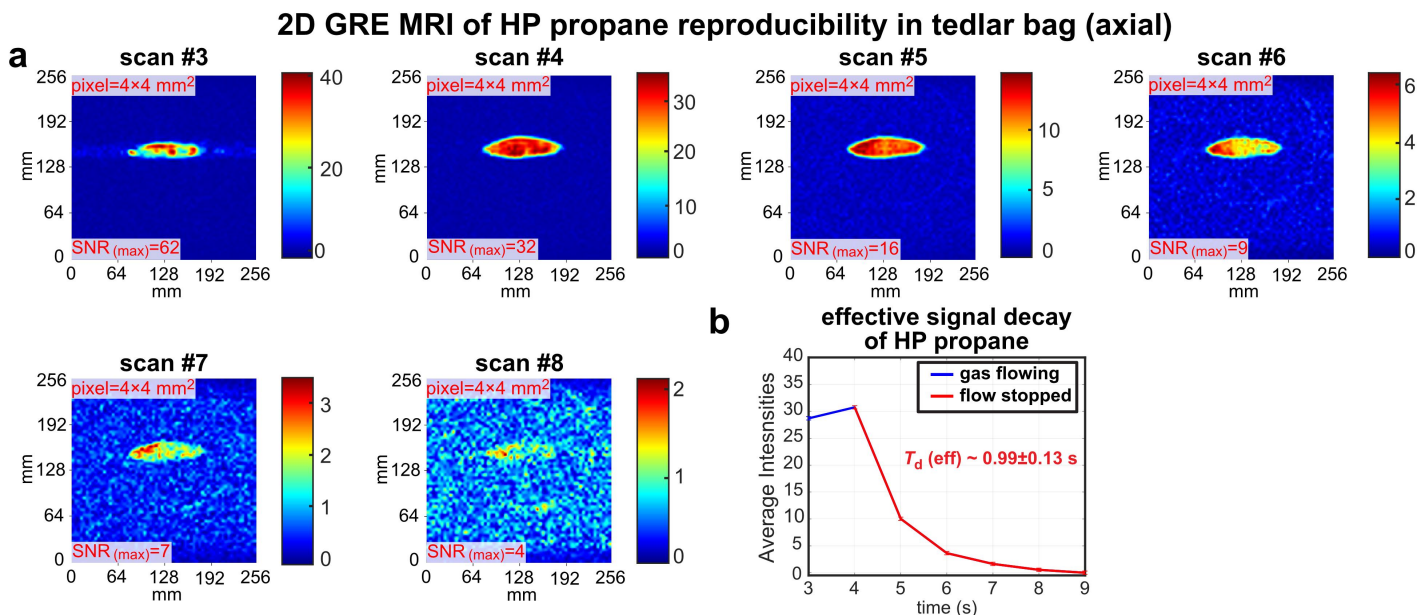


**Figure S8.** Sub-second slice-selective 2D GRE axial images of HP propane gas injected in a one-liter Tedlar bag and recorded with  $64 \times 64$  imaging matrix (converted to  $256 \times 256$  in post image processing) covering a  $256 \times 256$  mm<sup>2</sup> FOV, 50-mm slice thickness, and  $30^\circ$  slice-selective RF pulse. a) Intensity color-mapped images, tracking the changing dynamics of HP propane gas before, during and after HP gas ejection inside the Tedlar bag. To quantify the image quality, SNR were calculated via taking the highest-intensity matrix element from a  $3 \times 3$  matrix in highest intensity of the inflated region and a random RMS noise region. b) Average intensities of HP propane over time. Average intensities calculated from  $3 \times 3$  matrix average from highest intensity region before the gas flow was stopped and averages are taken from exactly the same position during the relaxation. The last 5 data points during the HP gas relaxation (gas flow stopped) were used to measure the effective  $T_d$  signal decay constant of  $0.99 \pm 0.13$  seconds using the model of mono-exponential decay.

#### d) Axial S14 HP propane MRI scanning (axial propane reproducibility run 2)

We have run the repeat of the reproducibility study of HP propane axial 2D GRE MRI described in the main text. The image series depict the temporal evolution of HP propane during its injection (scan #3), when became fully stopped (scan #4) followed by the decay of HP signal due to the compounding effect of the spin relaxation and excitation RF pulses. A total 16 scans were recorded, each slice represents  $\sim 0.97$  sec. The injection of HP gas was definitely stopped at scan #4. Therefore, HP state signal could only decay at slice scan #4 and after. As a result, the  $T_d$  was measured using the following difference images intensity: (scan #4 – scan #16), (scan #5 – scan #16), (scan #6 – scan #16), (scan #7 – scan #16), (scan #8 – scan #16) and , (scan #9 – scan #16). Effective  $T_d$  was found to be  $0.91 \pm 0.01$  seconds.

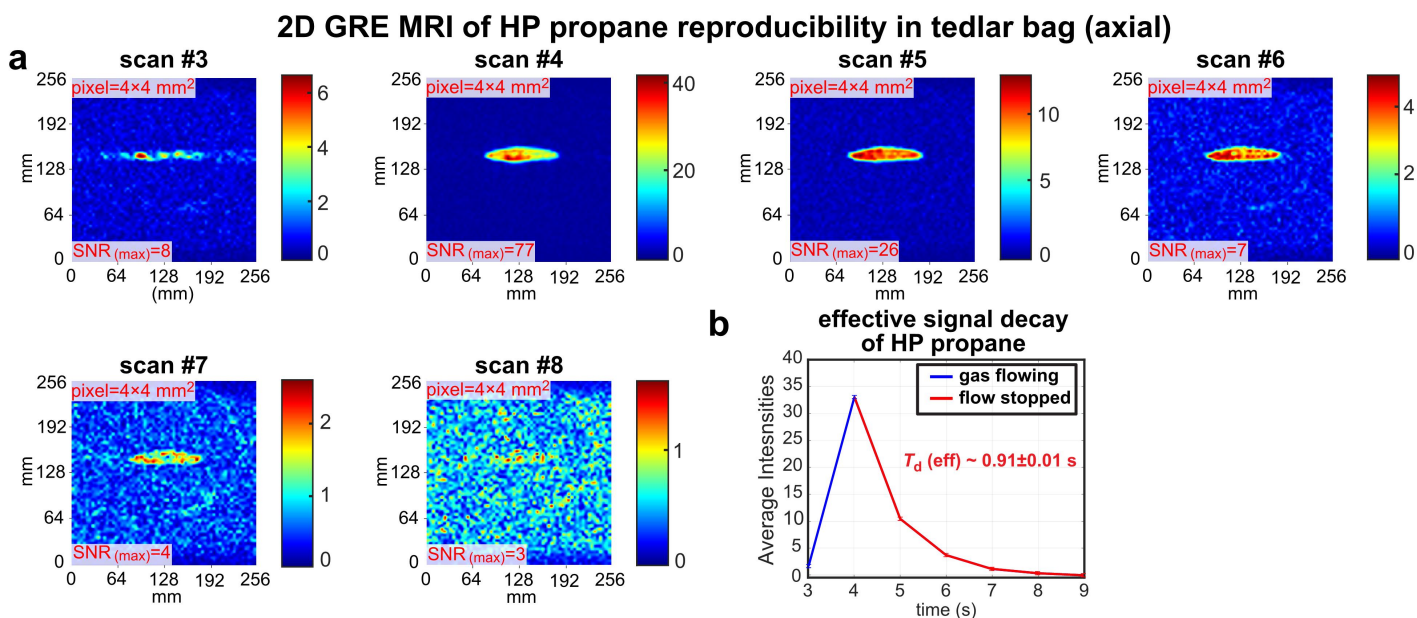


**Figure S9.** Sub-second slices-selective 2D GRE axial images of HP propane gas injected in a one-liter Tedlar bag and recorded with  $64 \times 64$  imaging matrix (converted to  $256 \times 256$  in post image processing) covering a  $256 \times 256$  mm<sup>2</sup> FOV, 50-mm slice thickness, and 30° slice-selective RF pulse. a) Intensity color-mapped images, tracking the changing signal dynamics of HP propane gas before, during and after HP gas ejection inside the Tedlar bag. To quantify the image quality, SNR were calculated via taking the highest-intensity matrix element from a  $3 \times 3$  matrix in highest intensity of the inflated region and a random RMS noise region. b) Average intensities of HP propane over time. Average intensities calculated from  $3 \times 3$  matrix average from highest intensity region before the gas flow was stopped and averages are taken from exactly the same position during the relaxation. The last 5 data points during the HP gas relaxation (gas flow stopped) were used to measure the effective  $T_d$  signal decay constant of  $0.91 \pm 0.01$  seconds using the model of mono-exponential decay.

### e) Coronal S29 HP butane MRI scanning (coronal butane run 1)

We have run the HP butane coronal 2D GRE MRI, scan #5 of which is presented in **Figure 4f**. The image series depict the temporal evolution of HP butane during its injection (scan #4), when became fully stopped (scan #5) followed by the decay of HP signal due to the compounding effect of the spin relaxation and excitation RF pulses. A total 16 scans were recorded, each slice represents  $\sim 0.97$  sec. The injection of HP gas was definitely stopped at scan #5. Therefore, HP state signal could only decay at slice scan #5 and after. As a result, the  $T_d$  was measured using the following difference images intensity: (scan #5 – scan #16), (scan #6 – scan #16), (scan #7 – scan #16), and (scan #8 – scan #16). Effective  $T_d$  was found to be  $0.82 \pm 0.05$  seconds.

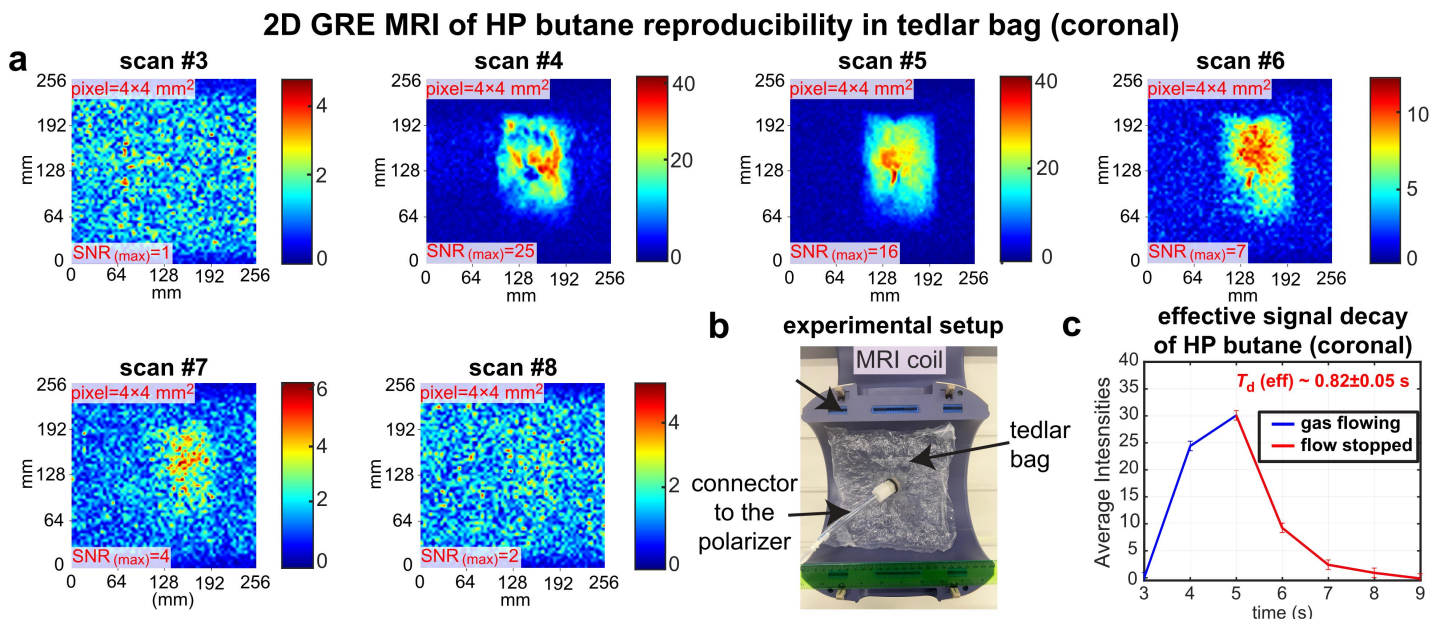


**Figure S10.** Sub-second slice-selective 2D GRE coronal images of HP butane gas injected in one-liter Tedlar bag and recorded with  $64 \times 64$  imaging matrix (converted to  $256 \times 256$  in post image processing) covering a  $256 \times 256$  mm<sup>2</sup> FOV, 50-mm slice thickness, and  $30^\circ$  slice-selective RF pulse. a) Intensity color-mapped images, tracking the changing signal dynamics of HP butane gas before, during and after HP gas ejection inside the Tedlar bag. To quantify the image quality, SNR were calculated via taking the highest-intensity matrix element from a  $3 \times 3$  matrix in highest intensity of the inflated region and a random RMS noise region. b) An annotated closeup photograph provides insight to the experimental configuration, highlighting the unmounted knee MRI coil from top view, connection to the polarizer and the Tedlar bag, with a ruler for scale. c) Average intensities of HP butane over time. Average intensities calculated from  $3 \times 3$  matrix average from highest intensity region before the gas flow was stopped and averages are taken from exactly the same position during the relaxation. The last 4 data points during the HP gas relaxation (gas flow stopped) were used to measure the effective  $T_d$  signal decay constant of  $0.82 \pm 0.05$  seconds using the model of mono-exponential decay.



### f) Coronal S30 HP butane MRI scanning (coronal butane reproducibility run 1)

We have run the reproducibility study of HP butane coronal 2D GRE MRI. The images depict the temporal evolution of HP butane. The image series depict the temporal evolution of HP butane during its injection (scan #4), when became fully stopped (scan #5) followed by the decay of HP signal due to the compounding effect of the spin relaxation and excitation RF pulses. A total 16 scans were recorded, each slice represents  $\sim 0.97$  sec. The injection of HP gas was definitely stopped at scan #5. Therefore, HP state signal could only decay at slice scan #5 and after. As a result, the  $T_d$  was measured using the following difference images intensity: (scan #5 – scan #16), (scan #6 – scan #16), (scan #7 – scan #16), and (scan #8 – scan #16). Effective  $T_d$  was found to be  $0.91 \pm 0.12$  seconds.

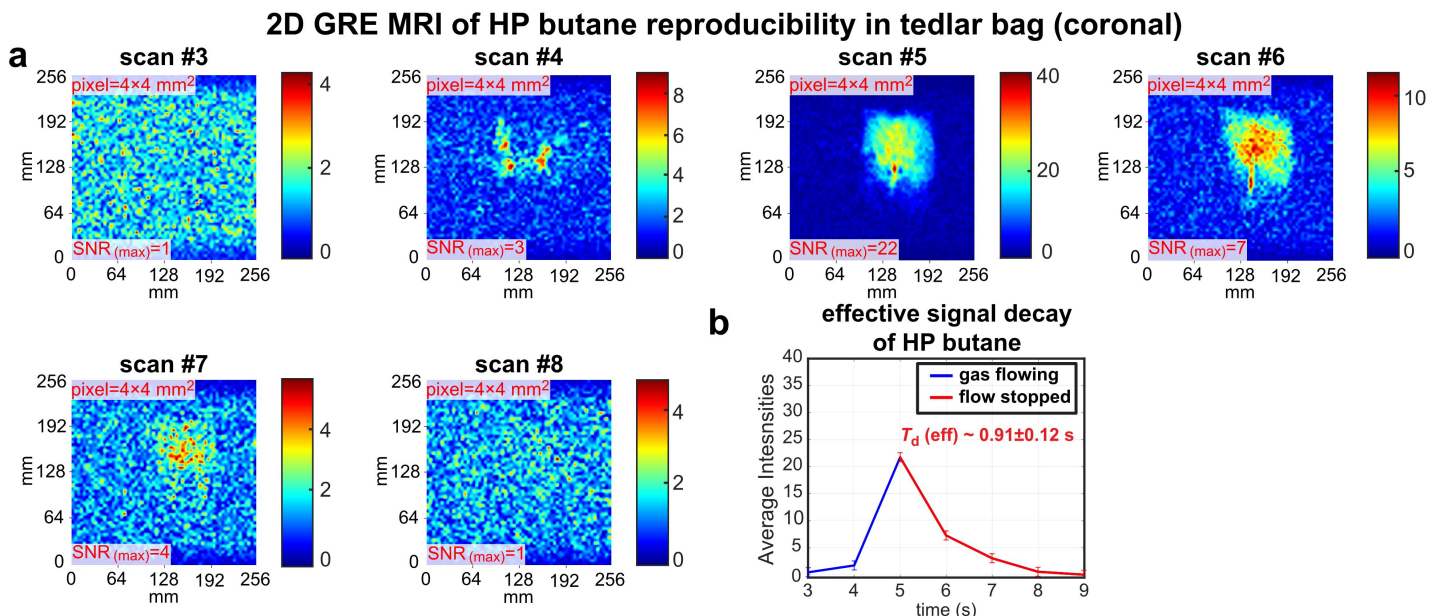


**Figure S11.** Sub-second slice-selective 2D GRE coronal images of HP butane gas injected in one-liter Tedlar bag and recorded with  $64 \times 64$  imaging matrix (converted to  $256 \times 256$  in post image processing) covering a  $256 \times 256$  mm<sup>2</sup> FOV, 50-mm slice thickness, and  $30^\circ$  slice-selective RF pulse. a) Intensity color-mapped images, tracking the changing signal dynamics of HP butane gas before, during and after HP gas ejection inside the Tedlar bag. To quantify the image quality, SNR were calculated via taking the highest-intensity matrix element from a  $3 \times 3$  matrix in highest intensity of the inflated region and a random RMS noise region. b) Average intensities of HP butane over time. Average intensities calculated from  $3 \times 3$  matrix average from highest intensity region before the gas flow was stopped and averages are taken from exactly the same position during the relaxation. The last 4 data points during the HP gas relaxation (gas flow stopped) were used to measure the effective  $T_d$  signal decay constant of  $0.91 \pm 0.12$  seconds using the model of mono-exponential decay.

### g) Coronal S11 HP propane MRI scanning (coronal propane run 1)

We have run the study of HP propane coronal 2D GRE MRI. The image series depict the temporal evolution of HP propane signal during its injection (scan #4), when became fully stopped (scan #5) followed by the decay of HP signal due to the compounding effect of the spin relaxation and excitation RF pulses. A total 16 scans were recorded, each slice represents  $\sim 0.97$  sec. The injection of HP gas was definitely stopped at scan #5. Therefore, HP state signal could only decay at slice scan #5 and after. As a result, the  $T_d$  was measured using the following difference images intensity: (scan #5 – scan #16), (scan #6 – scan #16), (scan #7 – scan #16), and (scan #8 – scan #16). Effective  $T_d$  was found to be  $0.78 \pm 0.04$  seconds.

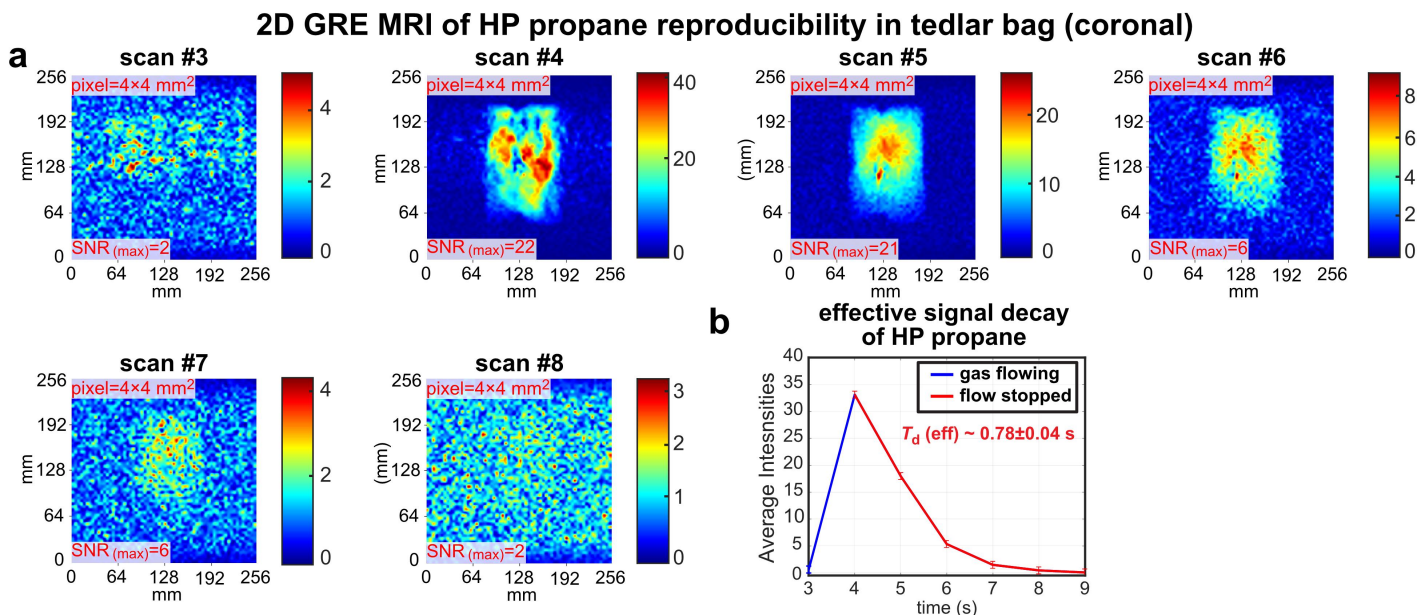


**Figure S12.** Sub-second slice-selective 2D GRE coronal images of HP propane gas injected in one-liter Tedlar bag and recorded with  $64 \times 64$  imaging matrix (converted to  $256 \times 256$  in post image processing) covering a  $256 \times 256$  mm<sup>2</sup> FOV, 50-mm slice thickness, and 30° slice-selective RF pulse. a) Intensity color-mapped images, tracking the changing signal dynamics of HP propane gas before, during and after HP gas ejection inside the Tedlar bag. To quantify the image quality, SNR were calculated via taking the highest-intensity matrix element from a  $3 \times 3$  matrix in highest intensity of the inflated region and a random RMS noise region. b) Average intensities of HP propane over time. Average intensities calculated from  $3 \times 3$  matrix average from highest intensity region before the gas flow was stopped and averages are taken from exactly the same position during the relaxation. The last 4 data points during the HP gas relaxation (gas flow stopped) were used to measure the effective  $T_d$  signal decay constant of  $0.78 \pm 0.04$  seconds using the model of mono-exponential decay.

### h) Coronal S13 HP propane MRI scanning (coronal propane reproducibility run)

We have run the reproducibility study of HP propane coronal 2D GRE MRI. The image series depict the temporal evolution of HP propane signal during its injection (scan #4), when became fully stopped (scan #5) followed by the decay of HP signal due to the compounding effect of the spin relaxation and excitation RF pulses. A total 16 scans were recorded, each slice represents  $\sim 0.97$  sec. The injection of HP gas was definitely stopped at scan #5. Therefore, HP state signal could only decay at slice scan #5 and after. As a result, the  $T_d$  was measured using the following difference images intensity: (scan #5 – scan #16), (scan #6 – scan #16), (scan #7 – scan #16), and (scan #8 – scan #16). Effective  $T_d$  was found to be  $0.81 \pm 0.07$  seconds.

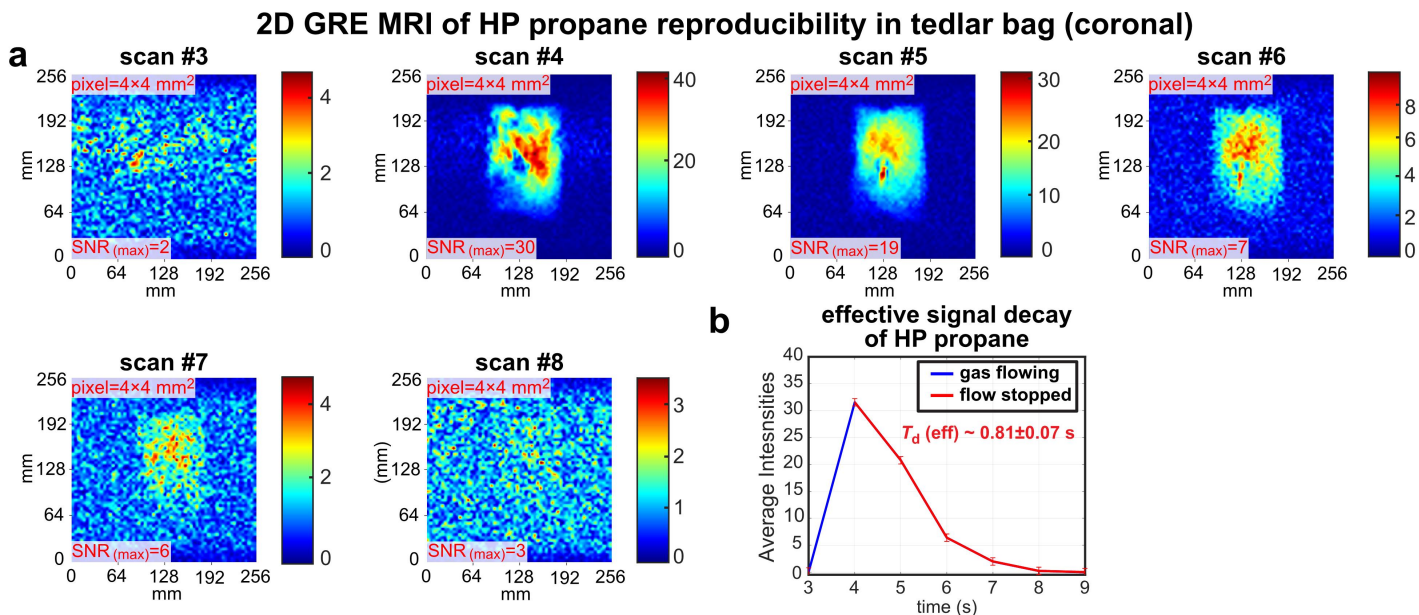


**Figure S13.** Fast slices-selective 2D GRE coronal images of HP propane gas injected in one-liter Tedlar bag and recorded with  $64 \times 64$  imaging matrix (converted to  $256 \times 256$  in post image processing) covering a  $256 \times 256$  mm<sup>2</sup> FOV, 50-mm slice thickness, and  $30^\circ$  slice-selective RF pulse. a) Intensity color-mapped images, tracking the changing signal dynamics of HP propane gas before, during and after HP gas ejection inside the Tedlar bag. To quantify the image quality, SNR were calculated via taking the highest-intensity matrix element from a  $3 \times 3$  matrix in highest intensity of the inflated region and a random RMS noise region. b) Average intensities of HP propane over time. Average intensities calculated from  $3 \times 3$  matrix average from highest intensity region before the gas flow was stopped and averages are taken from exactly the same position during the relaxation. The last 4 data points during the HP gas relaxation (gas flow stopped) were used to measure the effective  $T_d$  signal decay constant of  $0.81 \pm 0.07$  seconds using the model of mono-exponential decay.

## 8. Additional ventilation images of HP butane injected in rabbit lungs

We have also shown the feasibility of even higher resolution HP butane gas imaging in excised rabbit lungs (compared to that shown in the main text) by decreasing the pixel size down to  $1.6 \times 1.6 \text{ mm}^2$  using both axial and coronal projections, albeit at the expense of SNR, **Figure S14**.

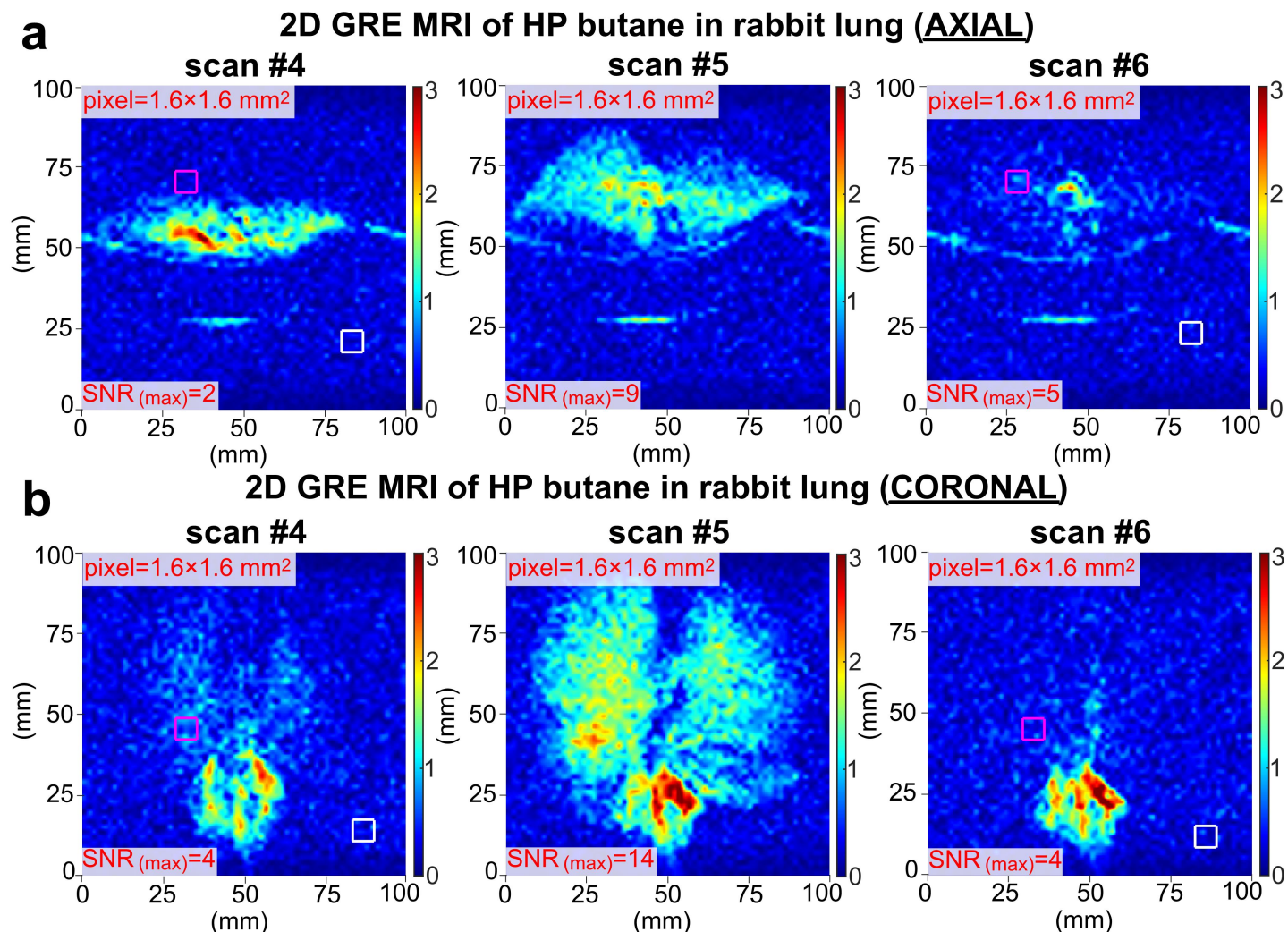


**Figure S14.** Sub-second slice-selective 2D GRE color images of HP butane gas injected in the rabbit lungs and recorded with  $64 \times 64$  imaging matrix (converted to  $256 \times 256$  in post image processing) over  $100 \times 100 \text{ mm}^2$  FOV, 50-mm slice thickness, and  $30^\circ$  slice-selective RF pulse. a) Time series of axial scans recorded before lungs' inflation with the HP butane (scan #4), at inflation (scan #5), after the inflation (scan #6), and the subtracted image obtained by subtracting the "scan #6" from "scan #5" image (to remove the background signals from surrounding tissues). b) corresponding time series recorded on a different HP butane gas injection in the same lungs in the coronal projection. The SNR<sub>(MAX)</sub> values were obtained by selecting the highest intensity pixel from the inflated lung region in scan #5 from  $3 \times 3$  matrix (shown by magenta box; the position of the box was kept the same for all images in series) in the highest intensity region and dividing it by RMS noise (obtained as an RMS value of the pixels from  $3 \times 3$  matrix elements in the noise region, shown by a white box; the position of the box was kept the same for all images in series).

## 9. 0.35 T MRI image analysis of HP gases

### Data extraction from MRI computer station

All acquired data extracted from the dedicated MRI station computer using a flash drive. One complete set of experiments in the MRI scanner can run up to 40 individual scans. All HP butane and propane images were taken using 16 repetitions as described in the main text. All these 16 scans for an individual run are saved inside folder named S(X), X=number of sequences. DICOM files are saved as I000000M (M=scan number).

### Post processing

#### I) File storage format and architecture

This section of the SI presents and discusses the currently utilized format for file and folder naming of MRI image analysis using MATLAB processing software. To ensure reproducibility between data sets, it is expected that data from all experiments is saved in a uniform fashion. After transferring the image data as DICOM file format from the MRI computer, the user selects a sequence with 16 scans that is under investigation. For example, S28 is a scan that used for acquiring axial HP butane images that is used in the **Figure SX**. Copy this file to a new analysis folder named “HP butane Axial S28 Data Analysis”. The folder should contain:

##### Axial HP Butane S28 Data Analysis

- SX (X=number of scan)
  - N number of DICOM files, Where N represents number of scans (16) used during the experiment.
  
- Difference Combination
  - [Image\\_Combination\\_Analysis.mat](#) file to analyze all the differences in scan s from 1 to 16 (e.g., 1-2, 1-3, 1-4,...) using colormap for different intensities.
  - **subtration.pdf** (Multiple PDF outputs of scans subtraction combination, with each containing 16 figure)
  
- $T_1$  Mapping
  - [Axial\\_S28\\_Td\\_Map.mat](#)
  - Find SNR before image subtraction.
  - “Difference image of selected signal and noise region.pdf” (generated to show the region selected region for noise and signal average)
  - “Average of SNR vs scan difference.pdf”
  - “Td Map” (PDF, contains  $T_d$  map of last 5 scan s (4-16, 5-16, 6-16, 7-16, 9-16) to measure the  $T_d$  signal decay).
  - Convert 64×64 raw images to 256×256 images.

#### II) MATLAB Data Analysis Protocol

This section of the supplementary information provides a comprehensive presentation and discussion of the complete automated data analysis protocol implemented in MATLAB. The protocol entails utilizing custom-built functions specifically designed for processing and analyzing data in the DICOM file format. It is assumed that the reader possesses a fundamental understanding of typical MATLAB functions, operations, and workflow.

Throughout the section, variable names and directories will be denoted within quotation marks, such as “Image\_Subtraction”. in-line comments are incorporated to enhance comprehension of the script's structure and operation. These comments are denoted by the % symbol in MATLAB and are displayed in green font to distinguish them from the code itself. An example of an in-line comment is `%this is a comment`.

### a) Image\_Combination\_Analysis.mat

In this section of the code, it generates all possible combinations of image subtraction using scans 1 to 16, where the presence of the hyperpolarized (HP) butane gas contrast agent is expected. During the experimental sequence, the process was initiated, and a 2-second delay was introduced (totaling 2 scans) before the HP contrast agent begin filling the Tedlar bag. With the continuous flow of HP gas, an additional 1 second (corresponding to time needed for recording 1 images) were required to completely fill the bag.

The comprehensive analysis of scans 1 to 16 provides a thorough evaluation of the experimental results of interest. Notably, the gas flow ceased approximately at scan 4, and the HP contrast agent has an approximate reported  $T_d$  value of  $1.04 \pm 0.24$  (see the details below). Consequently, scan 16 represents the inflated Tedlar bag without any HP agent present. This confirmation is derived from the analysis of the differences observed in the various combination comparisons. By examining these differences, we can establish the absence of the HP contrast agent in scan 16, validating its role as a reference for inflated Tedlar bag without any HP contrast.

```
% Clear the workspace and command window
clc;
clear;

% Specify the file paths for the DICOM images
filePaths = {
    'C:\ file_path_to_folder \I0000001.dcm',
    'C:\ file_path_to_folder \I0000002.dcm',
    'C:\ file_path_to_folder \I0000003.dcm',
    'C:\ file_path_to_folder \I0000004.dcm',
    'C:\ file_path_to_folder \I0000005.dcm',
    'C:\ file_path_to_folder \I0000006.dcm',
    'C:\ file_path_to_folder \I0000007.dcm',
    'C:\ file_path_to_folder \I0000008.dcm',
    'C:\ file_path_to_folder \I0000009.dcm',
    'C:\ file_path_to_folder \I0000010.dcm',
    'C:\ file_path_to_folder \I0000011.dcm',
    'C:\ file_path_to_folder \I0000012.dcm',
    'C:\ file_path_to_folder \I0000013.dcm',
    'C:\ file_path_to_folder \I0000014.dcm',
    'C:\ file_path_to_folder \I0000015.dcm',
    'C:\ file_path_to_folder \I0000016.dcm'
};

% Number of DICOM files
numFiles = numel(filePaths);

% Read the DICOM images
images = cell(1, numFiles);
for i = 1:numFiles
    images{i} = dicomread(filePaths{i});
end

% Create combinations for image subtraction
combinations = nchoosek(1:numFiles, 2);
numCombinations = size(combinations, 1);

% Set the maximum number of subplots per figure
maxSubplots = 16;

% Calculate the number of figures required
numFigures = ceil(numCombinations / maxSubplots);

% Counter for the current combination
combinationCounter = 1;
```

```

% Define the colormap
cmap = jet;

% Loop over the figures
for figureIndex = 1:numFigures
    % Create a new figure
    figure;

    % Set the title of the figure
    sgtitle(sprintf('Image Subtraction: %d - %d, %d - %d, ...', ...
        combinations(combinationCounter, 1), combinations(combinationCounter, 2), ...
        combinations(combinationCounter + 1, 1), combinations(combinationCounter + 1, 2)))%,
    'FontSize', 2);

    % Calculate the number of subplots for this figure
    numSubplots = min(maxSubplots, numCombinations - combinationCounter + 1);

    % Loop over the subplots in the current figure
    for subplotIndex = 1:numSubplots
        % Calculate the current combination index
        currentCombinationIndex = combinationCounter + subplotIndex - 1;

        % Compute the subtraction image
        subtracted_image = double(images{combinations(currentCombinationIndex, 1)}) -
double(images{combinations(currentCombinationIndex, 2)});

        % Create a subplot and display the image with colormap
        subplot(4, 4, subplotIndex);
        imshow(subtracted_image, []);
        colormap(cmap);
        colorbar;
        title(sprintf('Image %d - Image %d', combinations(currentCombinationIndex, 1),
            combinations(currentCombinationIndex, 2)));
        % Set the color map range from -2000 to 2000
        caxis([-2000, 2000]);
    end

    % Increment the combination counter
    combinationCounter = combinationCounter + numSubplots;

    % Save the figure as a PDF file
    exportgraphics(gcf, sprintf('subtraction_%d.pdf', figureIndex), 'ContentType',
'vector');
end

```

## b) Axial\_S28\_Td\_Map.mat

Upon conducting an analysis using the previous code, Image\_Combination\_Analysis.mat, it has been determined that the region of interest for the HP injection spans from scan 2 to scan 7. To further investigate this region, it is necessary to develop a code that individually computes the highest intensity matrix in the inflated lung region and RMS value of the random noise region to find the real SNR from the image matrix.

Then the differences between scan 2 and scan 16, scan 3 and scan 16, scan 4 and scan 16, scan 5 and scan 16, scan 6 and scan 16, as well as scan 7 and scan 16 is determined as assigned as new matrixes. The resulting difference images are saved in PDF file format. Two 3x3 black rectangle is drawn in the region that is selected to double check by the user for the highest intensity and noise region. Noise RMS is taken from each scans noise region and averaged it to get the error bar which is used to plot the points during the  $T_d$  relaxation measurement.

For  $T_d$  signal decay measurement, scans 4, 5, 6, and 7 were selected for measuring the  $T_d$  value inside the Tedlar bag. These scans were chosen as they represent a suitable region (selected as the region with definitive signal in all nine pixels; averaging is performed to boost SNR) for accurate  $T_d$  assessment. By analyzing the  $T_d$  values in this region, we can gain insights into the relaxation characteristics of the HP contrast agent after the gas ejection in Tedlar bag.

Moreover, to improve visual clarity and appeal all the subtracted images are resized to a dimension of 256x256 pixels from original 64x64 pixels. This resizing ensures that the images fit within a standardized visual space.

```
% Specify the paths of the 8 DICOM files
dicomPaths = {
    'C:\ file_path_to_folder \I0000002.dcm',
    'C:\ file_path_to_folder \I0000003.dcm',
    'C:\ file_path_to_folder \I0000004.dcm',
    'C:\ file_path_to_folder \I0000005.dcm',
    'C:\ file_path_to_folder \I0000006.dcm',
    'C:\ file_path_to_folder \I0000007.dcm',
    'C:\ file_path_to_folder \I0000016.dcm'
};

% Read the DICOM files
dicomFiles = cell(7, 1);
for i = 1:7
    dicomFiles{i} = dicomread(dicomPaths{i});
end
%%

% SNR Calculations
Images = cell(7, 1);
highestSignals0 = zeros(7, 1);
Image_averages = zeros(7, 1);

for i = 1:7
    Images{i} = double(dicomFiles{i});
    neighborhood0 = Images{i}(26:26, 26:28);
    neighborhood1 = Images{i}(10:12, 10:12);
    % Calculate the maximum from the 3x3 matrix of the signal
    max_signal_intensity = max(neighborhood0(:));
    %Calculate the rms noise
    noiserms = (rms(neighborhood1));
    noiserms1 (i) = (rms(noiserms));
    % Calculate SNR and store it in the array
    SNR (i) = (max_signal_intensity /noiserms1 (i));
end
% Create a subplot to plot all the difference images
```



```

figure;
for i = 1:7
    subplot(2, 4, i);
    imshow(Images{i}, []);
    colormap(jet);
    colorbar
    title(sprintf('SNR %d', i));

    % Highlight the selected 4x4 region
    hold on;
    rectangle('Position', [35, 27, 3, 3], 'EdgeColor', 'black', 'LineWidth', 2);
    rectangle('Position', [10, 10, 3, 3], 'EdgeColor', 'red', 'LineWidth', 2);
    hold off;
end

% Define the x-axis labels
xLabels = cell(7, 1);
for i = 1:7
    xLabels{i} = sprintf('%d-%d', i+5, 14);
end

% Define the last three data points for fitting
xData = [0.97, 2*0.97, 3*0.97, 4*0.97, 5*0.97, 6*0.97, 7*0.97];
yData = SNR(1:end);
xData=(xData)';
yData=(yData)';

% Fit the data to the T1 function: SNR = A * exp(-TE / T1)
f = fit(xData, yData, 'exp1');

%Determine fitting coefficients, max and uncertainty
coeffs = coeffvalues(f);
max=coeffs(1);
bounds = confint(f);
yErr = abs((bounds(1,1)-bounds(2,1))/2);

%Determine relaxation rate constants and uncertainty
T1val = abs(1/coeffs(2));
xErr = abs(1/bounds(1,2)-(1/bounds(2,2)))/2;

%Determine constants and uncertainty
maxtxt = num2str(max);
T1valtxt = num2str(T1val);
yErrtxt = num2str(yErr);
xErrtxt = num2str(xErr);

%Concatenate strings to generate buildup & fit characteristics
fiteqtxt = 'y = a*exp(bx)';
coefftxt = strcat('a = ', num2str(coeffs(1)), ' b = ', num2str(coeffs(2)));
figtxt1 = strcat('max = ' + " " + maxtxt + " " + '+/-' + " " + yErrtxt);
figtxt2 = strcat('T_1 = ' + " " + T1valtxt + " " + '+/-' + " " + xErrtxt + " " + 'Secs');

% Plot the SNR values against the number of differences
figure;
plot(f, 'r--', xData, yData, 'ks');
xlabel('Time (s)');
ylabel('SNR Averages');
title('SNR Averages vs Time');

```

```

legend('Data', 'Exponential Fit');
xpos = (1);           %adjust this if buildup doesn't reach
ypos = (1);           %steady state (may overlap plot)
text(2.5*xpos,12*ypos,figtxt1)
text(2.5*xpos,10*ypos,figtxt2)
grid on;

% Save the figure as a PDF file
saveas(gcf, 'SNR.pdf');

%%
% Subtract each image from the 7th image
subtractedImages = cell(7, 1);
highestSignals = zeros(7, 1);
averages = zeros(7, 1);

for i = 1:7
    subtractedImages{i} = double(dicomFiles{i}) - double(dicomFiles{7});

    % Find the two highest values in the matrix
    sortedValues = sort(subtractedImages{i}(:), 'descend');
    secondHighestValue = sortedValues(2);

    % Find the row and column indices of the second highest value
    [rowIndices, colIndices] = find(subtractedImages{i} == secondHighestValue);

    % Select a 3x3 neighborhood around the second highest value if valid indices exist
    if ~isempty(rowIndices) && ~isempty(colIndices)
        rowIndex = rowIndices(1);
        colIndex = colIndices(1);

        % Check if the indices are within the valid range
        if rowIndex > 1 && rowIndex < size(subtractedImages{i}, 1) && colIndex > 1 && colIndex <
size(subtractedImages{i}, 2)
            neighborhood = subtractedImages{i}(24:26, 39:41);

            % Calculate the average of the neighborhood
            average = abs(mean(neighborhood(:)));

            % Store the second highest signal and average for the current matrix
            highestSignals(i) = secondHighestValue;
            averages(i) = average;
        end
    end
end

% Display the highestSignals and averages matrices
disp('Highest Signals:');
disp(highestSignals);
disp('Averages:');
disp(averages);

% Display the highestSignals matrix
disp(highestSignals);

% Create a subplot to plot all the difference images

```

```

figure;
for i = 1:7
    subplot(2, 4, i);
    imshow(subtractedImages{i}, []);
    colormap(jet);
    colorbar
    title(sprintf('Difference %d', i));

    % Highlight the selected 3x3 region
    hold on;
    rectangle('Position', [39, 24, 3, 3], 'EdgeColor', 'black', 'LineWidth', 2);
    hold off;
end

% Save the figure as a PDF file
saveas(gcf, 'Difference Images for Td Selected region.pdf');

%%
% Define the x-axis labels
xLabels = cell(7, 1);
for i = 1:7
    xLabels{i} = sprintf('%d-%d', i+2, 16);
end

noisermsavg=(78.32+90.42+81.51+77.53+77.59+80.06)/6;
% Create an array for error bars with a constant value of 24.71
errorBars = ones(size(averages)) * noisermsavg;

% Plot the matrix with error bars
figure;
errorbar(1:7, averages, errorBars, 'o-');
set(gca, 'YLim', [-50, 4000]);
set(gca, 'XTick', 1:7, 'XTickLabel', xLabels);
xlabel('Scan');
ylabel('Value');
title('Average Intensities vs Number of Differences');
grid on;

% Save the figure as a PDF file
saveas(gcf, 'Axial average VS Scan with Error Bars.pdf');

%%
% Define the last three data points for fitting
xData = [0.97, 2*0.97, 3*0.97, 4*0.97];
yData = averages(4:end);
xData=(xData)';
yData=(yData);

% Fit the data to the T1 function: SNR = A * exp(-TE / T1)
f = fit(xData, yData, 'exp1');

%Determine fitting coefficients, max and uncertainty
coeffs = coeffvalues(f);
max=coeffs(1);
bounds = confint(f);
yErr = abs((bounds(1,1)-bounds(2,1))/2);

```

```

%Determine relaxation rate constants and uncertainty
T1val = abs(1/coeffs(2));
xErr = abs(1/bounds(1,2)-(1/bounds(2,2)))/2;

%Determine constants and uncertainty
maxtxt = num2str(max);
T1valtxt = num2str(T1val);
yErrtxt = num2str(yErr);
xErrtxt = num2str(xErr);

%Concatenate strings to generate buildup & fit characteristics
fiteqtxt = 'y = a*exp(bx)';
coefftxt = strcat('a = ',num2str(coeffs(1)), ' b = ',num2str(coeffs(2)));
figtxt1 = strcat('max = ' + " " + maxtxt + " " + '+/-' + " " + yErrtxt);
figtxt2 = strcat('T_1 = ' + " " + T1valtxt + " " + '+/-' + " " + xErrtxt + " " + 'Secs');

% Plot the SNR values against the number of differences
figure;
plot(f, 'r--', xData, yData, 'ks');
xlabel('Time (s)');
ylabel('Averages');
title('Average Intensities vs Time');
legend('Data', 'Exponential Fit');
xpos = (1); %adjust this if buildup doesn't reach
ypos = (1); %steady state (may overlap plot)
text(2.5*xpos, 700*ypos, figtxt1)
text(2.5*xpos, 500*ypos, figtxt2)
grid on;

% Save the figure as a PDF file
saveas(gcf, 'Td MAP.pdf');

%%
% Create a subplot to plot all the difference images
figure;
for i = 1:7
    subplot(2, 4, i);
    imshow(imresize(subtractedImages{i}, [256, 256]), []); % Resize the image to 256x256
    colormap(jet);
    colorbar
    title(sprintf('Difference %d', i));

end

% Save the figure as a PDF file
saveas(gcf, 'Difference Images 256x256.pdf');

```

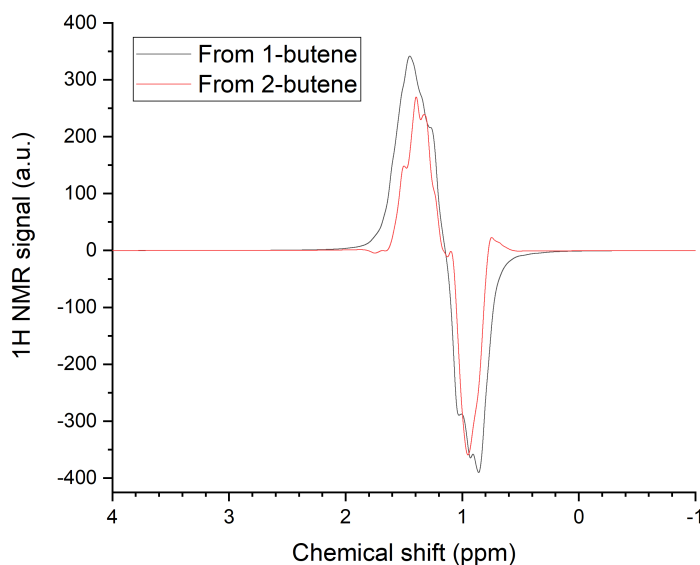


**Figure S15.** Simulated ALTADENA NMR spectra of products of pairwise p-H<sub>2</sub> addition to 1-butene and 2-butene precursors using NMR detection at 1.4 T using line broadening of 4 Hz. These simulations reveal overall lower intensity of HP butane ALTADENA spectra for the product of pairwise p-H<sub>2</sub> addition when 2-butene is employed as the to-be hydrogenated precursor versus that for 1-butene precursor.

## 10. Literature cited in supporting information (SI)

1. Ariyasingha, N. M.; Salnikov, O. G.; Kovtunov, K. V.; Kovtunova, L. M.; Bukhtiyarov, V. I.; Goodson, B. M.; Rosen, M. S.; Koptug, I. V.; Gelovani, J. G.; Chekmenev, E. Y. Relaxation Dynamics of Nuclear Long-Lived Spin States in Propane and Propane-d<sub>6</sub> Hyperpolarized by Parahydrogen. *J. Phys. Chem. C* **2019**, *18* (123), 11734–11744.
2. Joalland, B.; Nantogma, S.; Chowdhury, M. R. H.; Nikolaou, P.; Chekmenev, E. Y. Magnetic Shielding of Parahydrogen Hyperpolarization Experiments for the Masses. *Magn. Reson. Chem.* **2021**, *59* (12), 1180-1186.
3. Pravica, M. G.; Weitekamp, D. P. Net NMR Alignment By Adiabatic Transport of Parahydrogen Addition Products To High Magnetic Field. *Chem. Phys. Lett.* **1988**, *145* (4), 255-258.